



universität
wien

MASTERARBEIT

Titel der Masterarbeit

Late Cretaceous Volcaniclastic Rocks in the Pontides
(NW Turkey)

verfasst von

Katharina Böhm BSc

angestrebter akademischer Grad

Master of Science (M.Sc.)

Wien, 2015

Studienkennzahl lt. Studienblatt:

A 066 815

Studienrichtung lt. Studienblatt:

Erdwissenschaften

Betreuerin / Betreuer:

Ao. Univ.-Prof. Dr. Michael Wagreich

Declaration

"I hereby declare that this master's thesis was authored by myself independently, without use of other sources than indicated. I have explicitly cited all material which has been quoted either literally or by content from the used sources. Further this work was neither submitted in Austria nor abroad for any degree or examination."

Contents

Declaration	2
1. Introduction	8
1.1. Project	9
1.1.1. Goals	9
1.2. Geographical setting	10
1.3. Geological setting	12
1.3.1. The Pontides	14
1.3.2. The Pontides in the Cretaceous	18
1.3.3. Correlation with relative ages	24
2. Nomenclature	28
3. Methods	29
3.1. ICP-ES and ICP-MS	29
3.2. PXRD	29
3.3. Heavy mineral extraction	30
4. Results	31
4.1. Mineralogy	31
4.1.1. Powder X-Ray diffraction	31
4.1.2. Thin sections	33
4.1.3. Mineral Extraction: Dating of minerals	34
4.2. Geochemistry	36
5. Interpretation of the geochemical results	37
5.1. Mobility of elements	37
5.2. Alteration of minerals	39
5.3. Determining the rock type	41

5.4. Discriminating volcanic series	48
5.5. Revealing the tectonic setting	52
5.6. Plotting geochemical element patterns	60
5.7. Summary of the geochemical classification	62
6. Discussion	64
6.1. Correlation of geochemistry interpretation with the two volcanic formations	64
6.2. Geochemical studies on volcanoclastics in northern Turkey	65
6.3. Situation of the magmatic arc within the paleogeographic discussion	67
7. Outlook	69
8. Conclusio	70
9. Acknowledgements	71
List of Figures	72
List of Tables	74
Bibliography	75
A. Abbreviations	86
B. Tables	88

Preface

Volcaniclastic rocks are essentially igneous on the way up and sedimentary on the way down.

R. V. Fisher (cited in a presentation of Hudak, 2010)

Abstract

In the Late Cretaceous a bimodal volcanism developed in the recent area of the Western Pontides (NW Turkey). This volcanism can be traced in sections all along the Black Sea coast as distinct volcanoclastic layers. Successions include alternating successions of limestones, marls, turbidite and tuff. The middle Turonian to Santonian Lower Volcanic Succession (Dereköy Formation), the upper Santonian pelagic limestone (Unaz Formation) and the Campanian Upper Volcanic Succession (Cambu Formation) can be distinguished in this region. The successions were deposited under different stages of subduction of Tethys Ocean and contemporaneously spreading in the Western Black Sea basin. Rifting and spreading caused an extensional regime and formation of sedimentary basins along the southern shore of the Black Sea, in the Istanbul and Sakarya zones. To get a better correlation between cyclostratigraphy, biostratigraphy, tectonic setting and volcanic series, the volcanoclastics were classified by using a geochemical approach. As the volcanoclastic material is assumed to be deposited under subaqueous conditions, element mobility was important to consider when choosing element abundances and ratios for classification. Generally an overall trend of calc-alkaline to high K calc-alkaline series and basaltic to basalt andesitic rock types can be seen. A clear negative Nb anomaly with respect to Th and Ce in all samples excludes a within plate setting, and confirms the existence of a volcanic arc. This is also confirmed by a negative Ti anomaly. Normalized to normal mid-oceanic ridge basalt (N-MORB) the element variations show two types of volcanic arc basalts (VAB). The calc-alkaline to high-K calc-alkaline VAB have increased Nb and Zr values relative to N-MORB, whereas the tholeiitic VABs are depleted in Nb, Zr, Ti, V relative to N-MORB.

Zusammenfassung

Im heutigen Gebiet der Westlichen Pontiden (NW Türkei) trat in der Oberkreide bimodaler Vulkanismus auf. Charakteristische vulkanische Ablagerungen finden sich in zahlreichen Aufschlüssen entlang der türkischen Schwarzmeerküste. Die stratigraphischen Abfolgen umfassen Karbonate, Mergel, Turbidite und Tuffe. Es können die Untere Vulkanische Abfolge vom mittleren Turonium bis Santonium (Dereköy-Formation), die pelagischen Kalke vom oberen Santonium (Unaz-Formation) und Obere Vulkanische Abfolge vom Campanium (Cambu-Formation) unterschieden werden. Die Ablagerung erfolgte zeitgleich mit verschiedenen Stadien der Subduktion des Neotethys Ozeans und dem Aufgehen des Schwarzen Meers. Das Rifting und Spreading dieses neuen Meeresbeckens hatten ein Extensionsregime und die Bildung von Sedimentbecken entlang der südlichen Schwarzmeerküste in der Istanbul und Sakarya Zone zur Folge. Um eine Korrelation zwischen Zyklostratigraphie, Biostratigraphie, Paläotektonik und vulkanischen Ereignissen in der Oberkreide zu erreichen, wurden die Vulkaniklastika geochemisch charakterisiert. Das vulkanoklastische Material wurde unter hauptsächlich subaquatischen Bedingungen abgelagert, daher war die Beachtung der Mobilität von Elementen ein wichtiger Bestandteil bei der Auswahl der Elemente und Elementverhältnisse zur geochemischen Interpretation. Ein allgemeiner Trend von kalkalkalinen zu kaliumreiche kalkalkalinen Suiten und Basalten bis Basalt-Andesiten konnte festgestellt werden. Eine deutliche negative Nb-Anomalie zu Th und Ce in allen Proben schließt einen Intraplatten Ursprung aus und bestätigt einen vulkanischen Bogen. Dieser ist auch durch die negative Ti-Anomalie und durch zahlreiche Klassifikationsdiagramme bestätigt. Des Weiteren können die mit N-MORB normalisierten Kurven der Elementhäufigkeiten in zwei Gruppen von Basalten des Vulkanischen Bogens unterteilt werden. In kalkalkaline bis kaliumreiche kalkalkaline Basalte angereichert an Nb und Zr im Verhältnis zum N-MORB und mehr tholeiitische Basalte, die abgereichert sind an Nb, Zr, Ti und V im Vergleich zum N-MORB.

1. Introduction

Volcaniclastic layers within cyclic successions contain valuable information on the type of volcanism and volcanic events which created them. Geochemical analysis of the volcaniclastic material clarify properties of the volcanic source and therefore provide constrains on plate tectonic position and movement. Further, in stratigraphy volcano-genetic minerals of tuff layers can provide means for radiometric dating of sedimentary successions. This master thesis analysis volcaniclastic rocks within a Late Cretaceous Tethyan succession in northern Turkey. Sampled tuff layers, were between one and fifteen centimeters thick and were interbedded with marl, marly limestones, and some turbidites.

The main focus is on the geochemical and petrological characterization of the tuffs to get information on the overall tectonic setting and volcanism in the Late Cretaceous. Moreover, a correlation of the hereafter presented results with biostratigraphy, cyclostratigraphy and astronomical cycles from Upper Cretaceous successions can be done. Furthermore the geochemical characterization of the volcaniclastic material can be the base for future geochronological investigations. High-resolution absolute ages for the proposed paleotectonic setting would be in great demand.

The geochemical characterization of Upper Cretaceous volcaniclastic material from north-western Turkey helps to verify an existing or develop a new paleogeographic model of the Anatolia region in this time. Supported by discrimination diagrams the tectonic setting, dominated by subduction and fault zones, should be revealed further. In the northwestern part of Turkey, on the Black Sea coast good outcrop conditions were found to study long continuous Upper Cretaceous successions. Complete cyclic successions of the Campanian, the longest stage in Upper Cretaceous (83.6 ± 0.2 to 72.1 ± 0.2 Ma, IUGS Stratigraphic Chart 2014/10), are rare. The intention of the supporting project is to get a continuous cyclostratigraphic

record and astronomical time scale of the Tethyan Campanian to date environment changes. Neotethys subduction, Black Sea rifting and oceanic spreading, significant decrease in ocean temperature (e.g. [Pucéat et al., 2003](#)), increase in oxic conditions ([Hu et al., 2005](#); [Wang et al., 2011](#)), OAE, CORBS, sea level changes are some of the reasons why these results of the project form an important mosaic in understanding.

1.1. Project

This master thesis is part of a FWF project “Cyclostratigraphy and the astronomical time scale for the Tethyan Campanian (Late Cretaceous)”, which aims to correlate a new high-resolution cyclostratigraphic and multistratigraphic record for the Campanian of the Tethys with a astronomical target curve and will fundamentally help in achieving an absolute time scale and duration for the Late Cretaceous and the rapid environmental changes in paleoceanography and paleoclimatology (project proposal Wagreich, 2012).

1.1.1. Goals

The goal of this work is characterization of the volcanoclastic material of selected Upper Cretaceous sections in the Sinop-Boyabat basin in Turkey in terms of mineralogy and petrological geochemistry. The defined topic was on the mineralogy and geochemistry of tuff layers in the Campanian of the Pontides (Bartın and Amasra sections). Identification, logging and sampling of the tuff layers, sample preparation, whole rock geochemistry and if possible mineral separation for high accuracy geochronology were the assigned tasks. The study evolved and tasks were renamed. Geochronology could not be carried out on the existing samples because latter do not fulfill the requirements of the project. Aside from the mentioned tasks the overall aim of this work is to draw conclusions out of geochemical results and classify the volcanic rocks, rock types and volcanic series, to assign the type of volcanism and consequently the tectonic setting of eruption. The question to be answered is, whether if geochemical results can verify existing paleogeographic and tectonic models or not. The evolution of the Tethys in Late Cretaceous is of

course closely linked to this question. Together with other results from the framing project, this may be an approach to clarify tectonic and geographic settings of the multi-branched Tethys Ocean and the Anatolia region in Upper Cretaceous times.

1.2. Geographical setting

During this study Campanian volcanoclastics in the northern and central northwestern part of Turkey were sampled. One area is situated in the north of Turkey directly alongside the southern Black Sea coast. It is belonging to the Black Sea Region, which is one of seven regions in Turkey and which is divided into 18 provinces. Bartın, Kastamonu and Sinop Province are covering the study area. More precisely (road) sections along the coast, between Bartın, Amasra, Cide and İnebolu were investigated. The outcrop area lies within the Sinop-Boyabat basin.

The second study area within this project was in central northwestern Turkey, also in the Black Sea Regions, in the Bolu Province. This area is situated more to the south, going up-country. Samples were taken around Göynük, Mudurnu, Yenipazar and Nallihan, in the Mudurnu-Göynük basin.

GPS coordinates of the probed sections along the Black sea coast are listed in Table B.1 and the positions are highlighted in Fig. 1.1, in a Google Earth extract.

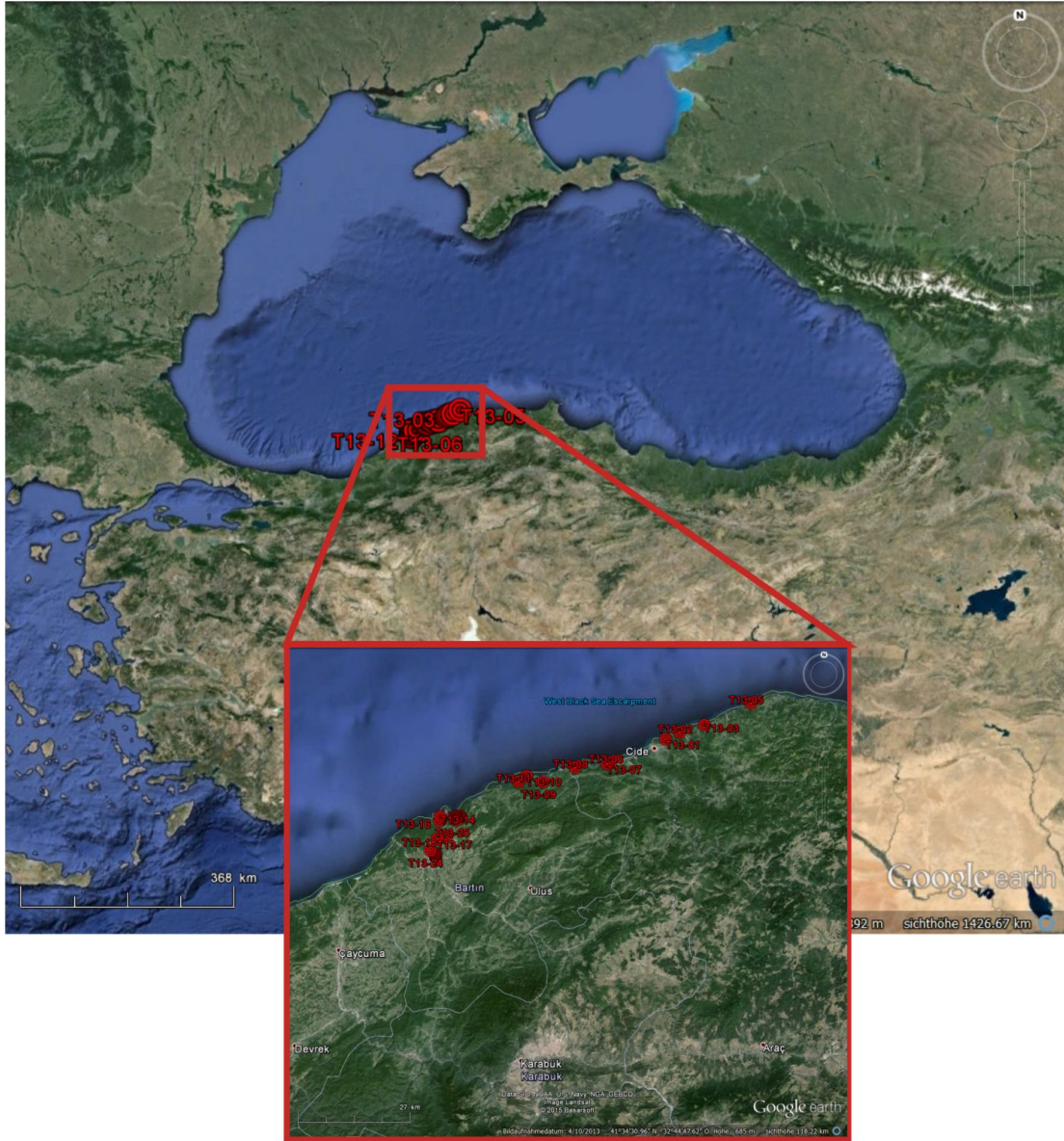


Figure 1.1.: Outcrops visited in the Western Pontides

1.3. Geological setting

The Geology of Turkey is closely linked to the evolution of the Tethyan Ocean. Since the Carboniferous the Tethys existed between the continents Laurussia in the north and Gondwana in the south (Stampfli and Borel, 2002). Tethys developed as a multi-branched ocean between several continental fragments, parts of them representing Turkey at present time, derived from the margin of the two mega-continents (e.g. Okay, 2008; Bozkurt and Mittwede, 2001). The existence of two ophiolitic sequences and accretionary prisms with different ages in Anatolia, thus two structural-rift-related distinguishable Tethyan Oceans, the Palaeo- and the Neotethys, is widely agreed on (e.g. Şengör and Yilmaz, 1981; Okay and Tüysüz, 1999; Stampfli, 2000; Bozkurt and Mittwede, 2001). The Mesozoic to early Cenozoic Neotethyan Ocean can be divided into three branches (e.g. Şengör and Yilmaz, 1981; Bozkurt and Mittwede, 2001). This model including the Intra-Pontide, the northern Neotethys and southern Neotethys ocean basin is sketched in Fig. 1.2. While part of the southern basin of the Neotethys is still preserved in the eastern Mediterranean Sea (Robertson, 1998; Stampfli and Borel, 2002; Garfunkel, 2004), most parts of the branched Tethys Ocean was consumed and subducted in several stages.

The subduction of Neotethys Ocean in this region is of part of controversial discussions in literature. While Robertson et al. (1996) suggest a northward subduction since the Paleozoic ongoing till the Eocene, Eyüboğlu et al. (2006, 2007), Eyüboğlu (2010) and Chorowicz et al. (1998) and others are favoring a continuous south dipping subduction polarity from the Paleozoic to the end of Eocene. In contrast Şengör and Yilmaz (1981), Tüysüz et al. (1995), Tüysüz (2011), Saribudak (1989), Hippolyte et al. (2010), Okay et al. (1994), Okay (2008), and others are arguing for a north dipping subduction zone from Late Cretaceous onwards till the end of Eocene.

Following the subduction the terranes collided (Şengör, 1985; Hempton, 1987) and were amalgamated during Alpine Orogeny (Okay, 2008). The suture zones between those continental fragments bear evidence for the different oceanic basins which divided them (Ketin, 1966; Şengör, 1987). The five main geologic units of Turkey are the Pontides, the Anatolides, the Taurus Cimmerian domain, the South-Taurides exotic units and the Arabian domain. The domains have different geo-

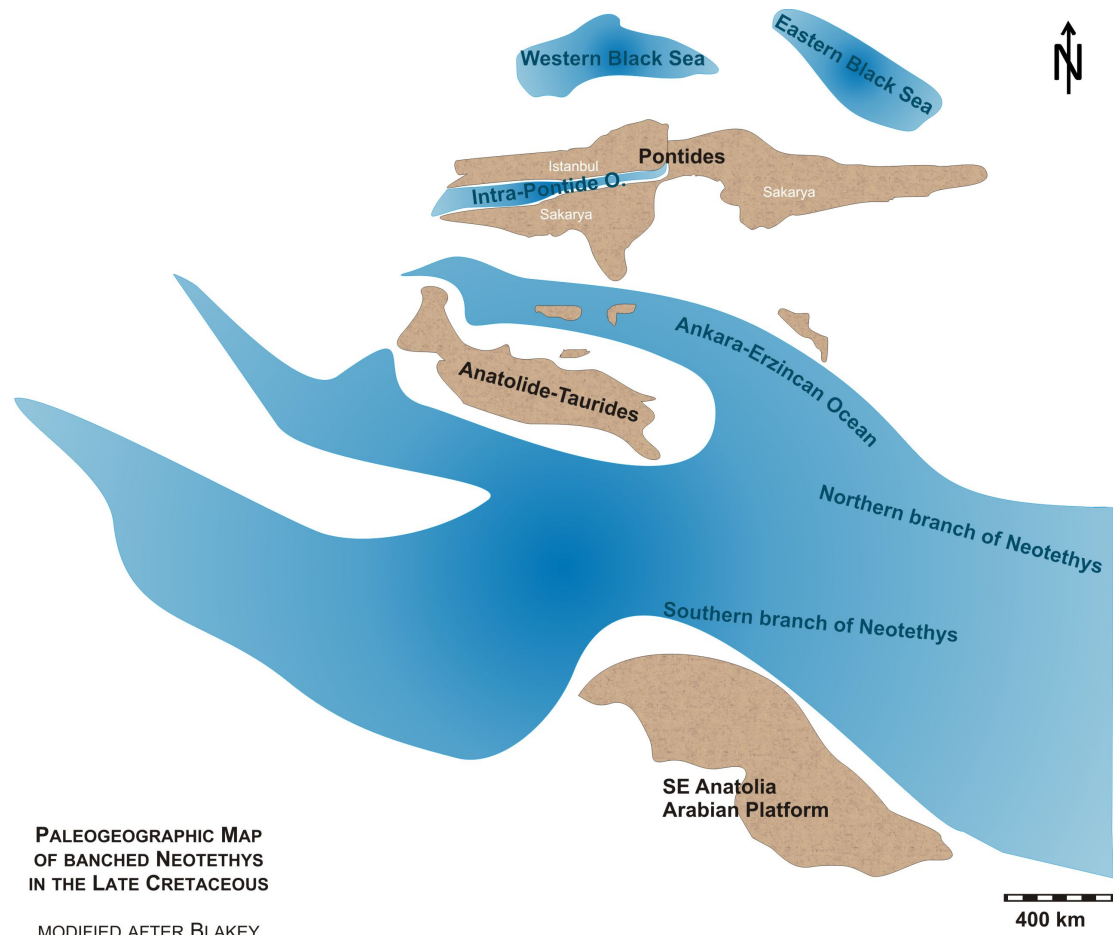


Figure 1.2.: Paleogeographic map of the branched Neotethys in the Late Cretaceous, modified from Blakey



Figure 1.3.: Insert of major geologic units (white), suture zones (turquoise) and faults (red) of Turkey in a Google Earth Image

dynamic evolution and are divided by suture zones (Stampfli, 2000; Stampfli and Borel, 2002; Moix et al., 2008; Okay, 2008). Further five major Tethyan suture zones were assigned by Okay and Tüysüz (1999), the Izmir-Ankara-Erzincan, Intra-Pontides, Inner Tauride, Antalya/Pamphyllan and South East Anatolian / Assyrian-Zagros suture zone. The geological units, suture zones and major recent faults are depicted in Fig. 1.3 and in the geologic map of turkey (Fig. 1.4).

1.3.1. The Pontides

The research area is situated in the Pontides, north of the Anatolides geologic unit. The Pontides itself are built up by fragments, belonging to Laurasia, accreted pro-

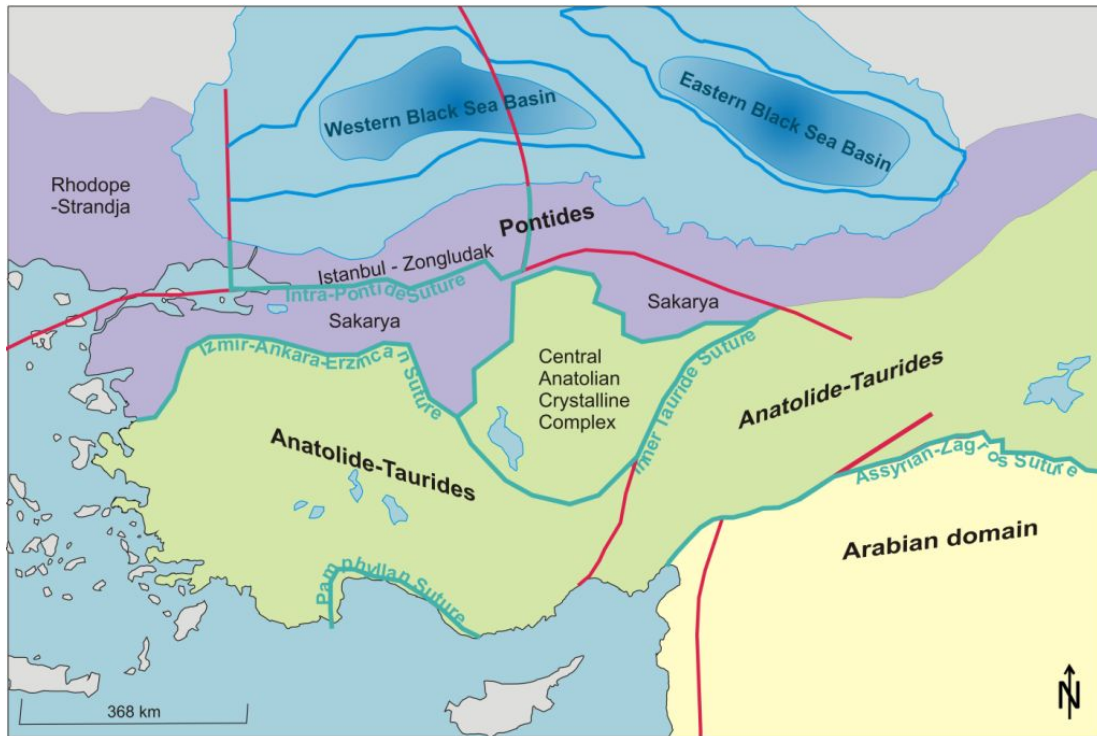


Figure 1.4.: Geologic map of Turkey, modified from Stampfli, 1998; Moix, 2008; Okay and Tüysüz, 1999

gressively since Triassic time. They were amalgamated in mid Cretaceous, following the subduction of the Neotethys under the Pontides in Early Cretaceous (Okay et al., 2006; Moix et al., 2008) the closure of the Intra-Pontide Ocean and the opening of the Black Sea. A magmatic arc from the Srednagorie Zone in Bulgaria to the Caucasus in Georgia (Tüysüz, 2011) developed in the Late Cretaceous and stayed active till Maastrichtian (e.g. Çoğulu, 1975; Karacık and Tüysüz, 2010). Evidence of Variscan and Cimmeride orogenies are preserved in the Pontides, as there is no major imprint of Alpine metamorphism (Okay, 2008). Only the Zonguldak zone was not affected by Variscan metamorphism.

The Pontides can be split up in three terranes, namely the Rhodope-Strandja, Istanbul-Zonguldak and Sakarya terrane (Şengör and Yilmaz, 1981; Okay and Tüysüz, 1999; Moix et al., 2008).

The Strandja zone is part of a large crystalline terrane, where also the Rhodopes are associated to. The Variscan basement, which is dominated by gneisses and late Carboniferous and early Permian intruded granitoids (Okay et al., 2001b) is

unconformably overlain by a Triassic to Jurassic sediment sequence. The Triassic part is characterized by Germanic Triassic facies with Lower Triassic clastic rocks and Middle Triassic shallow marine carbonates. Then around the Triassic to Jurassic boundary the Cimmeride deformation and metamorphism occurs. Allochthones developed in Jurassic and are unconformably overlain by middle Cretaceous shallow marine sandstones and Upper Cretaceous volcanogenic rocks which can be found all along the Pontides and even in Bulgaria in the Sredna–Gora zone (Okay et al., 2008).

The other two terranes, introduced hereafter, are containing the sampled areas. The Istanbul and Zonguldak zones are part of the Western Pontides, situated on the south-western margin of the Black Sea. The Precambrian basement, mainly exposed in the Bolu Massif, is unconformably overlain by an Ordovician to Carboniferous succession. The lower part is described as terrestrial to marine clastic, grading into a deeper marine succession in the west and shallower marine succession in the east (Haas, 1968; Görür et al., 1997). After the Variscan deformation and metamorphism, the stratigraphic difference between west and east can be still clearly seen (Okay et al., 2006). In the eastern part the Carboniferous is unconformably overlain by Triassic terrestrial succession, followed by a thick Middle Jurassic to Eocene shallow marine clastic succession. In the western part Jurassic and Lower Cretaceous sequences are missing and Paleozoic and Triassic sediments are unconformably overlain by Upper Cretaceous to Paleocene clastics, carbonates and volcanics (Okay et al., 2008). The Istanbul terrane is delimited by the Intra-Pontide suture zone to the south against Sakarya (Şengör and Yilmaz, 1981) and lies between two transform faults, the prolongation of the Western Black Sea Fault in the west and the West Crimean Fault/Arac-Dady-Inebolu shear zone in the east (Okay, 1989; Okay et al., 1994; Tüysüz, 1999). Paleotectonic models suppose that during Early Cretaceous the Istanbul terrane finally rifted away from Eurasia as a result of back-arc extension, created by northward subducting Neotethys. Then drifted southwards along the Western Black Sea and West Crimean Fault and collided in early Eocene with Sakarya terrane creating the Intra-Pontide suture zone. The location of the Istanbul terrane within the Pontides and the mentioned faults along which the fragment was supposed to be moved southwards can be seen in Fig. 1.5.

Sakarya terrane, also addressed as Central and Eastern Pontides, comprises vari-

able metamorphosed crystalline basements. There is a Carboniferous sequence with preserved Variscan high grade metamorphism, which is overlain by upper Carboniferous sediments. Further granitoids, with Devonian to Carboniferous or Permian crystallization ages, intruded and are uncomfortably overlain by Jurassic sediments (Okay et al., 2008).

Moreover, the Karakaya Complex, a Permo-Triassic low-grade metamorphic complex, is often referred as part of Sakarya terrane. It can be split up into the Lower Karakaya subduction-accretion Complex of Palaeozoic to Triassic Tethys Ocean (Tekeli, 1981; Pickett et al., 1996; Okay et al., 2001a), which comprises blueschists and eclogites probably originated from Laurussian margin, and Upper Karakaya Complex, which is made up of clastic, volcanic, chert and limestone blocks. Latter are suspected to be exotic blocks with Gondwana origin (Meijers, 2007).

Beginning in Early Permian accretion in eastern Sakarya started. Further, accretion of oceanic islands to the southern margin of Laurussia led to the Cimmeride Orogeny in Late Triassic to Early Jurassic. As signs of short localized deformation are found it can be rated as accretion rather than collision (Pickett et al., 1996; Okay et al., 2001a). With the end of Palaeotethyan subduction and accretion in Early Jurassic shallow marine sediments were deposited with angular unconformity over the Karakaya Complex and Variscan metamorphic and plutonic rocks. This Lower Jurassic and younger sediments show fluvial to shallow marine character. While the western part of Sakarya is dominated by shales and conglomerates, the eastern part is characterized by volcanoclastics intercalated with sandstones. In Late Jurassic to Early Cretaceous times limestone deposits continues and the regime in the eastern Pontides changed to deeper marine. In the middle Cretaceous, when the Alpine orogeny started, ophiolitic mélangé, deep sea sandstones and shales were sedimented in the eastern Pontides (Okay, 2008).

The northern branch of the Neotethys, called Ankara-Erzincan Ocean or Ankara-Yozgat-Erzincan Ocean, separated the Sakarya terrane and the Anatolide-Tauride block between Early Jurassic to Late Cretaceous and Miocene (Şengör and Yilmaz, 1981; Koçyigit, 1991; Görür, 1988). Till the Late Cretaceous a sedimentary prism developed on the southern continental passive margin of Sakarya continent (Koçyigit, 1991), then the southern margin of Sakarya became an active continental margin and magmatic arc-derived volcanics, pyroclastic and volcanoclastic sediments were deposited (Tüysüz et al., 1995). The Izmir-Ankara-Erzincan

suture zone resulted in the closure of the northern branch of the Neotethys and the collision of the Pontides and the Anatolide-Taurides in late Paleocene - early Eocene.

Anatolia is a single land mass since Oligocene-Miocene when terranes collided (Okay, 2008). Convergence of African, Arabian and Eurasian plate is still ongoing, as outlined by the extrusion of Anatolia of 20-30 mm/year to the west (Chorowicz et al., 1999; Mann, 2007). This tectonic escape of Anatolia onto the Mediterranean lithosphere is affected and triggered by the northward subduction of the Aegean-Cyprean Arc beneath the Anatolian plate and by different transform faults zones, which developed at about 5 Ma. (Dewey and Şengör, 1979; Şengör, 1985; Şengör et al., 2005; Hubert-Ferrari et al., 2002; Bozkurt and Mittwede, 2001). The dextral North Anatolian Fault Zone, the sinistral North East Anatolian Fault Zone and the sinistral East Anatolian Fault Zone merging into the sinistral Dead Sea Fault Zone are the major neotectonic structures, which partly developed on preexisting fabrics like the E-W trending horsts and grabens in Western Anatolia or the Intra-Pontides and Izmir-Ankara-Erzincan suture zones (Barka, 1992; Koçyigit, 1996; Armijo et al., 1999; Bozkurt and Mittwede, 2001).

1.3.2. The Pontides in the Cretaceous

South of the Sakarya terrane the northern branch of the Neotethys, the Ankara-Erzincan Ocean was situated, whereas in the north the Intra-Pontide Ocean separated Sakarya from the Istanbul terrane (Şengör and Yilmaz, 1981). Then the Ankara-Erzincan Ocean got into a north dipping subduction zone. This consumption of the Neotethys caused back arc extension, which itself triggered the southward movement of the Istanbul terrane. Behind the terrane in the Early Cretaceous rifting of the Western Black Sea basin started.

The origin and development of the Black Sea

Deep seismic reflection studies confirm the existence of two oceanic basins in the Black Sea, separated by a northwest trending Mid-Black Sea Ridge (Finetti et al., 1988; Robinson et al., 1996). The older Western Basin is eastwest orientated and

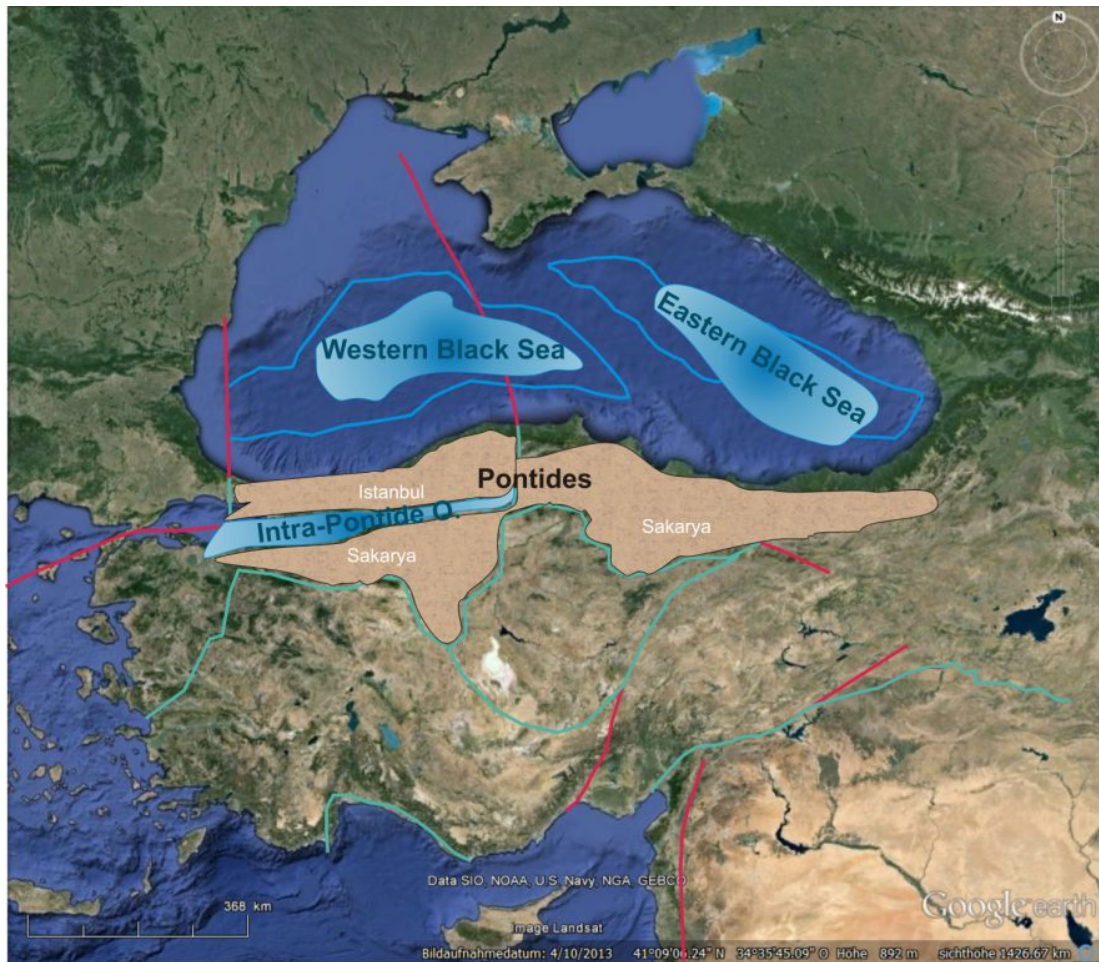


Figure 1.5.: Tectonic interpretation of the Turkey-Black Sea area, attention to Western and Eastern Black Sea basin, N-S trending Western Black Sea and West Crimean Fault (red), arrangement of the Pontides

has oceanic sea floor, whereas the eastern basin was rotated, is northwest orientated and shows oceanic or highly attenuated continental crust (Tüysüz, 1999). The older Western Black Sea basin is thought to be a back arc basin which started spreading in Late Cretaceous behind a volcanic island arc (Adamia et al., 1974; Hsü et al., 1977; Görür, 1988; Görür et al., 1997; Letouzey et al., 1977; Manetti et al., 1988). The Eastern Black Sea basin probably opened in Late Cretaceous and was extended during middle Eocene in a new cycle of volcanism, after the closure of the Intra-Pontide Ocean and the collisions of Sakarya with Istanbul terrane and Anatolide-Tauride block in early Eocene (Tüysüz, 1999).

Sedimentary basins alongside the Black Sea Coast

Due to an overall extensional regime in the north of the Pontides horst and graben thrust faults arised. Within these structures, on the southern margin of the Black Sea, on Istanbul and Sakarya terrane sedimentary basins developed in the Cretaceous (Fig. 1.6). In the eastern part of the Western Pontides the Zonguldak and Ulus basin developed, it was divided into two basins in Maastrichtian-Eocene, when sediments of the Devrek basin were deposited on top of Zonguldak basin. Also, in Late Cretaceous the Cide Upflift was elevated and was thrust over Devrek and Zonguldak after the middle Eocene. Another basin comprising the investigated Late Cretaceous sediments with Sakarya affiliation is the Sinop basin (Tüysüz, 1999).

The basins are mainly filled by Cretaceous sediments and volcanics. While the Lower Cretaceous units are different in the Istanbul and Sakarya basins, the Upper Cretaceous and younger records in Zonguldak, Ulus and Sinop basins are the same. The late- and post-magmatic sequences are very similar on Istanbul and Sakarya (Tüysüz, 2011).

The Zonguldak and Ulus basin on the Istanbul zone started to subside during the late Barremian, according to the sedimentary fill. The sediments in the east of the Istanbul zone represent late Barremian to Cenomanian opening and deepening periods, this development in the basins is probably contemporaneously with the opening of the Western Black Sea Basin. Latter was separated from the Zonguldak and Ulus basin by a short-lived carbonate platform. In Cenomanian a short period of uplift and erosion occurred and after this event, since late Cenomanian to Turo-

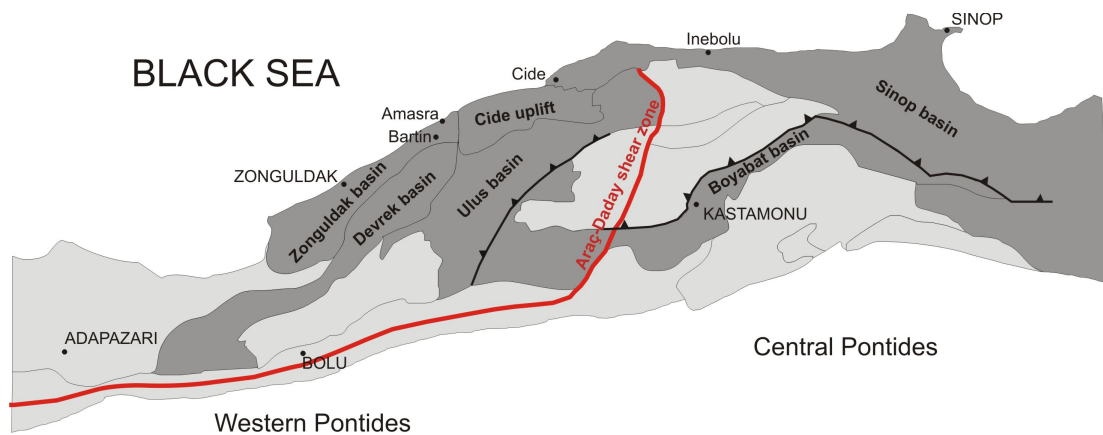


Figure 1.6.: Sedimentary basins in the Western and Central Pontides, modified from Tüysüz (2011)

nian sedimentation changed and extensive volcanism is recorded by volcanic and volcanoclastic deposits and alternating red pelagic shales and limestones (Tüysüz, 2011).

The basins belonging to Sakarya, in this case the Sinop Basin, mirror a horst-graben controlled opening and rapid deepening from late Barremian to Cenomanian. Between Cenomanian and Turonian deep marine red carbonates and shales were deposited (Tüysüz et al., 2012).

Late Cretaceous Volcanism in the Western Pontides

In the Late Cretaceous volcanism developed in northern Turkey (Fig. 1.7). It can be traced by volcanic deposits along the southern Black Sea shore and in north-western central Turkey, part of the Istanbul and Sakarya terrane (Cinku et al., 2009; Dewey et al., 1973; Nikishin et al., 2013; Tüysüz et al., 1995).

It is supposed that subduction of Neotethys, more precise subduction of the Ankara-Erzincan Ocean, lead to island arc volcanism in Late Cretaceous, which is referred to as the Pontides magmatic arc (e.g. Okay et al., 1994; Nikishin et al., 2003).

In the described area alongside the Black Sea coast three formations of Turonian to Campanian age can be distinguished (Fig. 1.8). Dereköy, Unaz and Cambu Formation are reflecting different stages of subduction of the Tethys as well as oceanic spreading in the Western Black Sea basin. According to Tüysüz (1999)

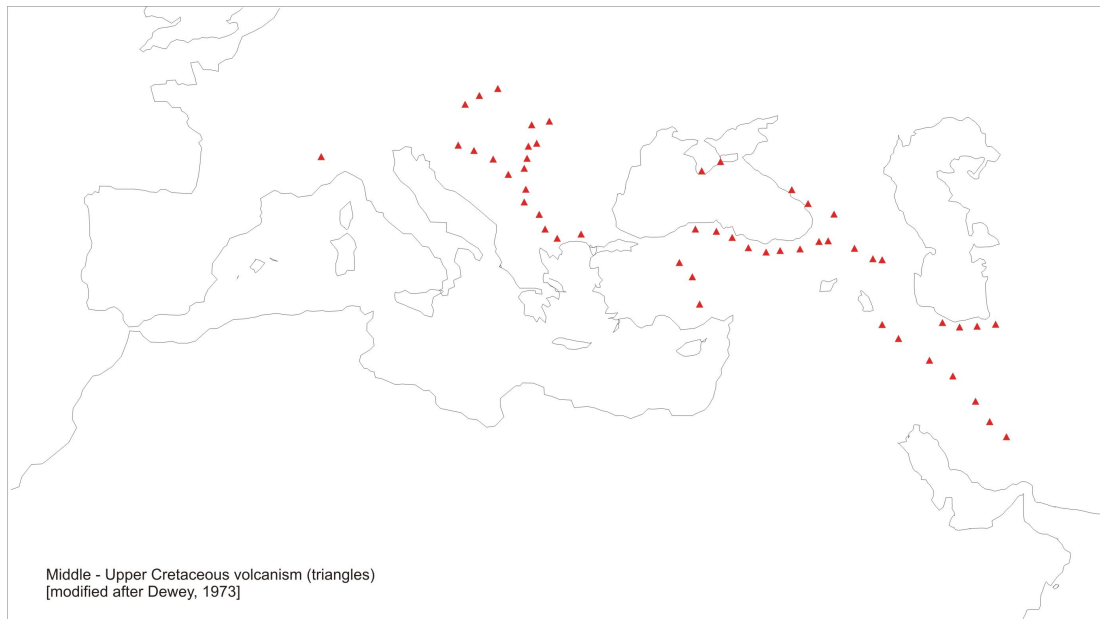


Figure 1.7.: Occurrence of middle to Late Cretaceous volcanism. Modified from Dewey et al., 1973

two different volcanic successions separated by Unaz Formation can be assigned in Late Cretaceous.

The first stage of volcanic activity in the Pontides, between Turonian to early Santonian is exhibited by the Lower Volcanic Unit, the Dereköy Formation (Tüysüz et al., 2012). The deposits of the Dereköy Formation start unconformable on Lower Cretaceous with a thick conglomerate and continue with intercalation of lavas, pyroclastics, turbiditic clastics, pelagic limestones and marls (Tüysüz et al., 2012). The general depositional environment is documented as a fast deepening realm. Late Cenomanian shallow marine carbonates were replaced in Turonian by pelagic carbonates (Tüysüz et al., 2012). This also confirms the extensional tectonic regime at that time. Occasionally blocks and debris flows created by normal faulting confirm extension. Following the extension of the basin igneous activity developed. Normal faulting and consequently horst and graben topography can be traced until the end of deposition of the Dereköy Formation. Sedimentary piles of the Lower Volcanic Unit are deposited mainly within the graben structures, whereas, after a period of subsidence, the Unaz Formation covers both, horst and graben (Tüysüz et al., 2012).

After sedimentation of the Unaz Formation the second volcanic cycle started. This

Upper Volcanic Succession is assigned as the Cambu Formation and was deposited throughout the Campanian. The second volcanic activity cycle is thought to have been more voluminous than the first one and is interpreted as post-rift deposit (Tüysüz, 2011). In the Cambu Formation basaltic and andesitic lava is interbedded with volcanoclastics and pelagic micritic limestones, similar to the Dereköy Formation (Tüysüz et al., 2012).







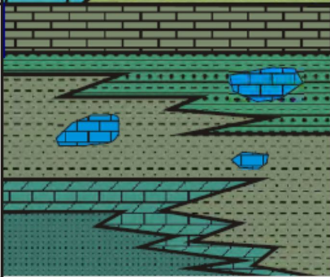
Age	Thickness (m)	Lithology	Formation
Eocene	>1000		Kusuri
Paleocene	50		Atbaşı
Maastrichtian	500		Akveren
Campanian	>1000		Cambu *
Campanian u. Santonian	20-200		Unaz
Coniacien Turonian	100-800		Dereköy * Yenice
Early Cretaceous	>1500 250 200 125		Cide Group

Figure 1.8.: Stratigraphy: Cambu and Dereköy Formation, sampled units are marked with *, modified from Tüysüz, 2011

1.3.3. Correlation with relative ages

Within the framing project relative ages are obtained through biostratigraphic methods. A correlation of these relative ages with the tuff samples allows an assignment of latter to the different formations. According to the position within stratigraphic successions six samples are associated to the Dereköy Formation. All others, despite T13/48/T which is part of the Maastrichtian Akveren Formation, are classified to the Cambu Formation based on occurrences of nannofossils and foraminifera.

Sample T13/03/T was taken from the Köseli section, is Coniacian in age and part

of the Dereköy Formation. The outcrop comprises micrites, shales and tuffs and is characterized through its steep inclined bedding (see also [Tüysüz et al., 2012](#)). The section near Kuscu comprises marly limestone - marl alterations with three interbedded tuff layers, which were sampled (T13/11b/T, T13/12/T, T13/12b/T). According to biostratigraphy it is of late Turonian to Santonian age and is therefore assigned to the Dereköy Formation as well. Whereas the section near Alayazi (T13/16/T) has lower to middle Campanian age and is thus referred to the older part of the Cambu Formation. The section investigated near Cayalti comprises cyclic pelagic marls and carbonates of early Santonian age, representing the Unaz Formation. The tuffs (T13/28/T, T13/30a/T, T13/30b/T) are overlying Unaz Formation and are therefore part of Cambu Formation, as there is no evidence of volcanism during deposition of Unaz Formation anywhere else. The mica rich tuff sample T13/34/T was taken east of Amasra, is interbedded between limestones and marls and belongs to the Dereköy Formation, according to occurrence of nannofossils. The outcrop near the village Kaman comprises limestones, shales and pyroclastics. The tuff layers were sampled (T13/37/T and T13/37b/T) and are assigned to the Cambu Formation. An alternating shale and limestone succession with tuff layers can also be found near Ugurlar. The sampled tuffs (T13/38/T, T13/39/T) are also inferred to be part of the Cambu Formation. Further the sample T13/40/T, from a small sandpit south-east of Amasra, belongs to the Upper Volcanic Succession as well. Sample T13/42/T belongs to the Dereköy Formation. The sampled tuff layer is overlying a limestone succession and a shale sequence rich in macro fossils. East of Bartın the Maastrichtian Akveren Formation comprises a thin calcite-altered tuff layer, which was sampled as well (T13/48/T).

Table 1.1.: Overview of sampled formations

Tuff samples			Assigned formation	Geographic description
T13/03/T			Dereköy	Köseli
T13/11b/T	T13/12/T	T13/12b/T	Dereköy	Kuscu
T13/16/T			Cambu	Alayazi
T13/28/T	T13/30a/T	T13/30b/T	Cambu	Cayalti
T13/34/T			Dereköy	E of Amasra
T13/37/T	T13/37b/T		Cambu	Kaman
T13/38/T	T13/39/T		Cambu	Ugurlar
T13/40/T			Cambu	SE of Amasra
T13/42/T			Dereköy	Amasra
T13/48/T			Akveren	East of Bartın

Late Cretaceous Volcanism in the Mudurnu-Göynük area

Additional to the basins alongside the Black Sea coast, some sections in the Mudurnu-Göynük basin were studied within this project. The “Mudurnu Trough” originated as an extensional rift basin on the Sakarya continental margin (Koçyigit, 1991). The Paleozoic basement representing Paleo-Tethys history (e.g. Okay and Tüysüz, 1999) is uncomfortably overlain by the Triassic metamorphic Karakaya Complex belonging to a marginal sea (Koçyigit, 1991). Then the Neo-Tethys development starts, seen in outcrops in the marginal areas of the basin as Lower Jurassic to Early Cretaceous transgressive succession, with alternating series of volcanics, shelf and pelagic carbonates as well as volcanoclastics. Those are consequently followed by deposits from the Late Cretaceous and Paleocene - early Eocene in the central part of the basin. The Upper Cretaceous pelagic carbonates represent progressive deepening of the depositional space from slope to basin environment. Turbiditic sequences are commonly deposited during this basin development, followed by red pelagic limestones and marls of the Santonian-Campanian, like those occurring in the Pontides. The marls are then again grading upwards into a Campanian to Maastrichtian turbiditic succession. The afore mentioned red limestones are part of the prominent cycle of deep marine sediments of alternating black shales and red beds from the Aptian to the Santonian (Yilmaz, 2008). Okay et al. (2001b) mentions tuff horizons in the Turonian - Santonian pelagic micrites. The Göynük Volcanoclastic Olistostrom representing the Göynük Formation (Köksal and Göncüoğlu, 1997; Köksal et al., 2001) is supposed to be Upper Cretaceous-

lower Paleocene ([Köksal and Göncüoğlu, 1997](#)). This olistostrom is of volcanosedimentary origin and has massive conglomerates at its base. The conglomerate is grain supported with clast sizes up to 15 cm and a volcanogenetic matrix. The components are rounded to sub-rounded volcanic, syenitic and consolidated shale pebbles ([Köksal and Göncüoğlu, 1997](#)). Further during field observations carbonate and chert pebbles were identified. The paleocurrent of this olistostrom towards south-east was determined according to imbrications of clasts and ripple marks on the base of the matrix dominated sequence at the base of the conglomeratic sequence. The olistostrom is thought to have been sedimented through subaqueous canyons within a fault controlled extensional basin ([Köksal and Göncüoğlu, 1997](#); [Köksal et al., 2001](#)).

2. Nomenclature

When it comes to nomenclature of ancient volcanoclastic rocks it is common in literature to use wide stretched terms of recent volcanoclastic classification. A good way for clear, non-ambiguous descriptions would be a nomenclature combining stage of alteration, lithofacies term, components and of course grain size (Fisher, 1961, 1966; McPhie et al., 1993). For instance some sampled rocks analyzed during this study could be addressed as smectite-altered, well sorted, crystal rich tuff. For reasons of comprehensive readability the altered tuff samples are often addressed general as volcanoclastics or tuffs only. According to Fisher and Schmincke (1984), tuffs are defined by grain size and pyroclastic content, but not by depositional environment. To be classified as tuffs grain size has to be smaller than 2mm, it has to be consolidated and has to contain more than three quarters of pyroclastics.

3. Methods

The methods used to achieve the goals of a mineralogical and geochemical characterization of the volcanoclastic materials are described in this chapter. On one hand analysis of whole rock geochemistry with ICP-MS, quantification of mineralogy by the use of PXRD and description of mineralogy and petrography with thin sections was done. On the other hand a range of different programs (mainly GCDkit, MinPet, IgPet, MS Excel) were used for interpretation of the data.

3.1. ICP-ES and ICP-MS

The whole rock geochemistry of 56 major and trace elements was carried out at the certified laboratory AcmeLabs Canada, Vancouver. A classical whole-rock analysis for 11 major oxides was carried out with ICP emission spectrometry, following a lithium borate fusion and dilute acid digestion. Samples were sintered at 1000°C (LOI) and Leco analysis for total carbon and sulfur was done. Determination of a 45-element suite of trace elements was performed using ICP mass spectrometry. Total abundances of rare earth and refractory elements were gained by lithium borate decomposition practice. Precious metals, base metals and their associated pathfinder elements were determined from an aqua regia digestion (AcmeLabs Canada). ICP-ES and ICP-MS techniques have precisions of 0.01% for oxides and 0.1-0.2‰ for trace elements, respectively.

3.2. PXRD

Bulk mineralogy was determined with powder X-ray diffraction at the University of Vienna. The samples were loaded into a sample holder as orientated powders.

Diffraction data were then collected with a Panalytical s X'Pert Pro diffractometer PW 3040/60), CuK α radiation (40 kV, 40 mA), step scan (step size 0.0167° 2 θ), 5s per step. The samples were run from 2 – 70° 2 θ . The x-ray diffraction patterns were interpreted using the Panalytical software X'Pert Highscore plus.

3.3. Heavy mineral extraction

Within the project an attempt was made to separate datable volcanic minerals out of the sampled tuff material. The suggested procedure was to extract heavy minerals and to test if suitable minerals for age dating were present. Loose sample material was put into acetic acid for seven days; organic material, carbonates etc. were dissolved at this stage, but unfortunately also, when present apatite. Afterwards a gravitational fluid (tetrabromoethane, 2.96 g/cm³) was used to separate heavy minerals like zircons or amphiboles.

4. Results

Mineralogical results from PXRD, thin sections and dateable heavy minerals and of course the geochemical results of the ICP-ES and ICP-MS analysis will be described in the following section.

4.1. Mineralogy

This section comprises summaries of the results of Powder x-ray diffraction, thin section and heavy mineral analyses .

4.1.1. Powder X-Ray diffraction

The mineralogical composition of the tuffs sampled in the Black Sea region between Bartın and Cide was investigated with powder x-ray diffraction (XRD). Almost all x-ray patterns (Fig. 4.1), except some of samples from Dereköy Formation, show feldspar peaks (3.18 Å). The alkali-feldspar sanidine and plagioclase (anorthite- albite) occur frequently, whereas the alkali-feldspar microcline was found less often. With increasing instability of anorthite (Ca-plagioclase), both calcite cement and clay mineral content increase, as documented by significant calcite peaks (3.03 Å) and clay mineral abundance. Clay minerals could be identified by a broad peak around 15 Å). Preferentially clay minerals of the expandable smectite group are represented by this peak and among these montmorillonite and nontronite are most common in volcanic rocks. After saturation of sample T13/30a with ethylene glycol, the peak at 15 Å) shifted to 17 Å); this confirmed the presence of smectite (Moore and Reynolds, 1989). Additionally some samples, mainly belonging to the Upper Volcanic Unit, show zeolite peaks (5.53 Å). They contain mainly analcime and

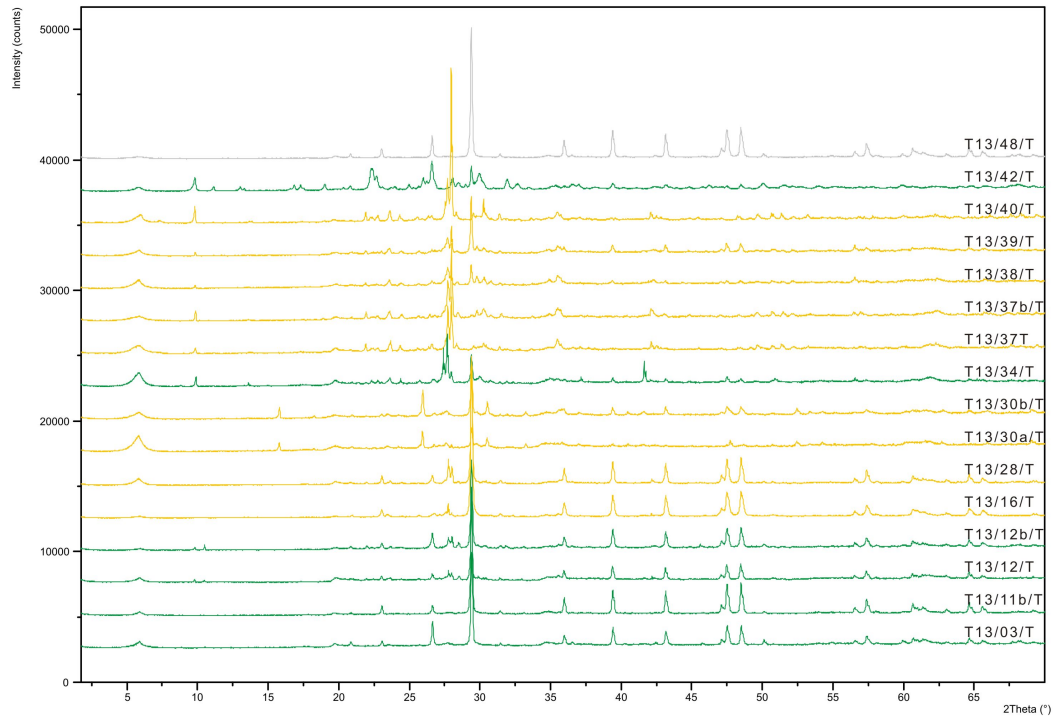


Figure 4.1.: Powder X-Ray diffractograms of the tuff samples from the Dereköy (green), Cambu (yellow) and Akveren (grey) Formation

clinoptilolite and smaller amounts of heulandite. In addition pyroxenes are found, augite is found in several samples (T13/30a, T13/37b, T13/42, T13/40). Amphiboles in contrast seem to be less abundant. Traces of actinolite are only found in some samples, one sample shows a distinctive hornblende peak (T13/12B). Additionally some samples contain magnetite minerals. Also quartz is abundant in seven samples, indicated by a peak at 3.34 \AA . In addition the quite significant background signal in some samples could represent the glassy matrix.

The results of the x-ray diffraction indicate some small differences between the samples from the Lower and Upper Volcanic Unit (Fig. 4.1). The majority of the samples from the Dereköy Formation contain quartz, whereas almost no quartz is present in those of the Cambu Formation. Further the Dereköy samples contain more calcite, but less feldspar. Zeolite minerals, like clinoptilolite are typical for the Cambu samples and could significantly less often be identified in the Dereköy samples.

4.1.2. Thin sections

Furthermore thin sections of the volcanoclastic rocks were investigated under the optical microscope (Fig. 4.2). In general the samples are fine grained, with crystal sizes below 1 mm. The tuffs contain lithic clasts, vitric clasts, as well as primary, secondary, matrix and cement minerals.

Lithic clasts are sub-rounded, are up to 2 mm in size and seem to be reworked volcanic rocks, having basaltic composition for example and comprising phenocrysts of plagioclase and sometimes pyroxene and titanomagnetite. Sometimes they are composed of an ashy matrix, embedding numerous crystal shards like plagioclase phenocrysts. In some cases the appearance reminds of the vesicular structure of pumice, which leads to the theory that cavities of pumice could be filled by secondary minerals forming the starting point for the observed assemblages. Especially rich in lithic fragments are the following investigated samples: T13/30b (Fig. 4.2 a), T13/34 (Fig. 4.2 b), T13/37, T13/37b.

Further vitric clasts are less abundant than the before described lithic clast, but still present in many samples. They have approximately the same size, often show narrow smectite rims and sometimes contain unaltered glass.

The observed crystal fragments are diverse, often embedded in finer grained matrix. Feldspar is abundant in all samples, predominantly plagioclase and the K-feldspar sanidine. Grain size and also preservation varies strongly. It ranges widely from big (up to 1 mm) euhedral to strongly fractured crystals to fine grained rims. In some thin sections the feldspars are especially big (Fig. 4.2 c), show traces of beginning breakdown, but are still idiomorphic, and can be described as micro-phenocrysts. One of the very feldspar rich samples is T13/11b (Fig. 4.2 d), with rather big euhedral, slightly rounded, and randomly orientated feldspars. In others big subhedral feldspar crystals are already partly decomposed, some of them still show zoning and only the ones with significant smaller grain size are still well preserved. In some samples are clearly dominated by elongated feldspar crystals (T13/37, Fig. 4.2 e).

The majority of the samples contain also carbonate minerals (Fig. 4.2 f), only in four samples no carbonate minerals were identified (T13/37, T13/37b, T13/39, T13/40). Calcite crystals as well as cement (T13/12b, T13/30b Fig. 4.2 f), rims

and veins (T13/30a) occur in the others. Glass is found in most samples, a significantly higher amount was noted in sample T13/37. Within altered glass relatively unaltered porphyric crystals are found. In some plagioclase crystals also glass inclusions were observed. Furthermore rounded and sometimes corroded quartz crystals with occasional oscillatory extinction are present. In many samples mica was found, ranging from euhedral biotites (T13/37, Fig. 4.2 e) to matrix forming mica (T13/34, T23/38). In quite a few samples thin section observations show preserved euhedral, rounded grains of olivine, partly decomposed. This abundance of olivine documents that alteration to chlorite, calcite, zeolite and analcime is in an early stage in these samples. In some samples amphiboles are found with a significant amount (T13/11b), in several also pyroxenes are abundant.

Lithic clasts, vitric clasts and crystals are embedded in a matrix of ash, glass, mica or other alteration minerals like clay. The different microscopic appearances of the samples ranged from commonly seen porphyric textures with some bigger clasts (T13/28, T13/38), dominating carbonate cement (T13/30b), deformed layers of fine grained minerals (T13/12b), “flow structures” (T13/37) to rather uniform coarse grained assemblages (T13/30b).

4.1.3. Mineral Extraction: Dating of minerals

Following the heavy mineral extraction treatment, zircons were only found in one sample, all others contained amphibole, pyroxene, olivine and mica. The zircon containing sample (T13/40) included clear, round, sedimentary zircons, as well as greenish, long prismatic, volcanic ones. But further treatment of the volcanic zircons was not carried out because a biostratigraphic correlation would not have been possible. The $^{40}\text{Ar}/^{39}\text{Ar}$ dating on sanidine or amphiboles was not tested as well, because of lack of accuracy (<0.5 Ma) needed for the project.

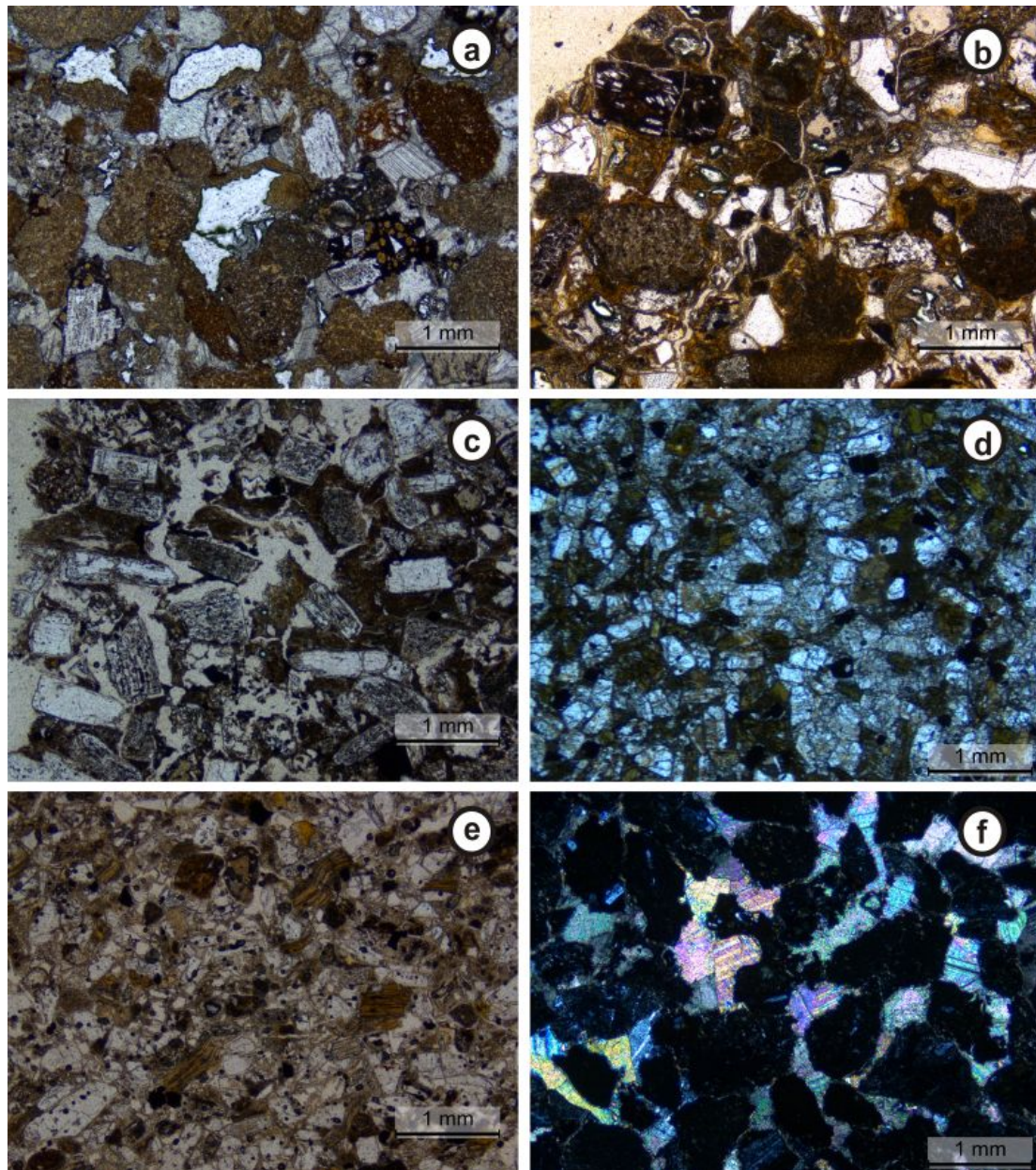


Figure 4.2.: Selected photomicrographs of the thin sections of volcaniclastic rocks from the SW Black Sea coast. (a) Vitric fragments (white) with glass inclusions; lithic fragments; carbonate minerals. (b) Lithic fragments, basalt clast with plagioclase and clinopyroxene crystals. (c) Large plagioclase phenocrysts; olivine (greenish); mica; lithic clasts. (d) Altered not-orientated feldspar crystals dominating. (e) Large mica aggregates (brown); fractured feldspars (bigger ones elongated); glass. (f) carbonate cement.

4.2. Geochemistry

The whole rock geochemistry results delivered by AcmeLabs Canada (Table B.2) are the starting point for any calculations and interpretation carried out. Numbers were recalculated on water free basis and then in the first steps alkali versus silica and normalized rare earth element abundances were plotted. Following element mobility estimations and tests, further discrimination diagrams were chosen. Further details will be discussed in the interpretation part, where selected element abundances and ratios were plotted and compared.

5. Interpretation of the geochemical results

The core of the study about the tuff layers are the geochemical analyses. The central questions, which should be answered by the interpretation of thereby gained results, are how to classify the volcanic rocks and in which tectonic setting they have been erupted. First one can be split in determination of the rock type and distinguishing between volcanic series. The tectonic setting revealed by geochemical discrimination can confirm palaeogeographic reconstructions or give new input to the discussions about subduction polarity, dating, marginal basins, accretions and collisions.

5.1. Mobility of elements

Prior to any evaluation or discrimination, the significance of the quantitative results was rated and clarified. As the sampled tuffs are Upper Cretaceous altered volcanic rocks, many processes have to be taken into account. Going back in time the question of deposition arises, whether it was a subaerial eruption with deposition into water or a submarine eruption and a form of subaqueous pyroclastic flow. Depositions were largely submarine, as deduced from intercalation with pelagic marl-marly limestone beds. Moreover, subaerial or subaqueous eruption type can be determined by paleogeographic reconstructions or by further investigations on well preserved volcanic deposits concerning vaporization in water and higher density and viscosity of aqueous environment relative to aerial. So if deposition was most likely under subaqueous conditions, the interaction with seawater has to be taken into account. Mobility of elements concerning formation of chlorides or other complexes seems not to be connected to the ionic potential, as long as the concentration of dissolved

species and the water-rock ratio is high (Pearce, 1996). Even, due to their intermediate ionic potential, rated immobile elements, form stable complexes under these mentioned conditions. Further, elements in basaltic glass like Y, P and rare earth elements can become mobile during intense sea-floor weathering (Murton et al., 1992; Price et al., 1991). Alteration could take place over a long time span since Upper Cretaceous and also subaerial weathering plays an important role. Types of leaching agents, redox potential, temperature, pressure and stability of minerals influences the behavior of elements during weathering have to be taken into account (Gouveia et al., 1993; Minařík et al., 1998; Nesbitt, 1979; Öhlander et al., 1996). Usually elements with intermediate ionic potential (charge/radius) are less affected by weathering as they tend to remain in the solid product and are the most immobile elements. Zr, Hf, Nb, Ta, Y, Ti, Cr, La, Th, Ga, Sc are some of the most immobile elements concerning weathering and metamorphism processes (Pearce, 1996) and can be therefore used to draw conclusions about mantle source, degree of melting, crustal level processes, differentiation and assimilation (Büchl and Gier, 2003).

However, testing of element mobility during alteration maybe useful. Cann (1970) (Fig. 5.1) developed bivariate variation diagrams. Elements to be evaluated are plotted on the vertical axis and a known immobile element is plotted on the horizontal axis. If the tested elements are moderately highly incompatible and immobile, trends with slopes close to unity should be displayed. Of course the samples used for correlation of incompatible elements have to be from one single lava suite and have to be split up into co-genetic groups. If latter is problematic, as genesis is not totally clear, like in our case, elements supposed to be immobile can be directly used for discrimination diagrams, and results have to be evaluated prior to interpretation to be not modified by alteration. Another useful test can be applied when plotting immobile element ratios, as latter are unlike influenced by alteration if the correlation coefficient is high (Pearce, 1996). But even “evidence of mobility does not always preclude the use of discrimination diagrams provided the alteration vectors are plotted” (Pearce, 1996, p 83).

5.2. Alteration of minerals

The sampled tuffs are not very resistant to alteration because they are not very consolidated and therefore highly porous. They show signs of alteration like secondary minerals, such as calcite, clay minerals and zeolites. Those minerals crystallized probably due to low temperature processes and processes like the circulation of fluids. This caused a change in original compositions indicated by the selective enrichment and depletion of major and trace elements. To determine the degree of alteration the abundance of certain clay minerals can be used. In a first stage, glass and olivine decompose to chlorite and also to calcite and zeolites. Afterwards chlorite will take up hydrated cations, which replace hydroxyl sheets. In addition corrensite will develop, which is composed of chlorite and vermiculite (Büchl and Gier, 2003). Also smectites form easily on basaltic materials as Fe-Mg species (Chamley, 1989). Consequently the degree of alteration can be deduced very accurately by the abundance of these clay minerals. In general it can be assumed that those samples are not too much altered as there are still some olivines and glass relics present.

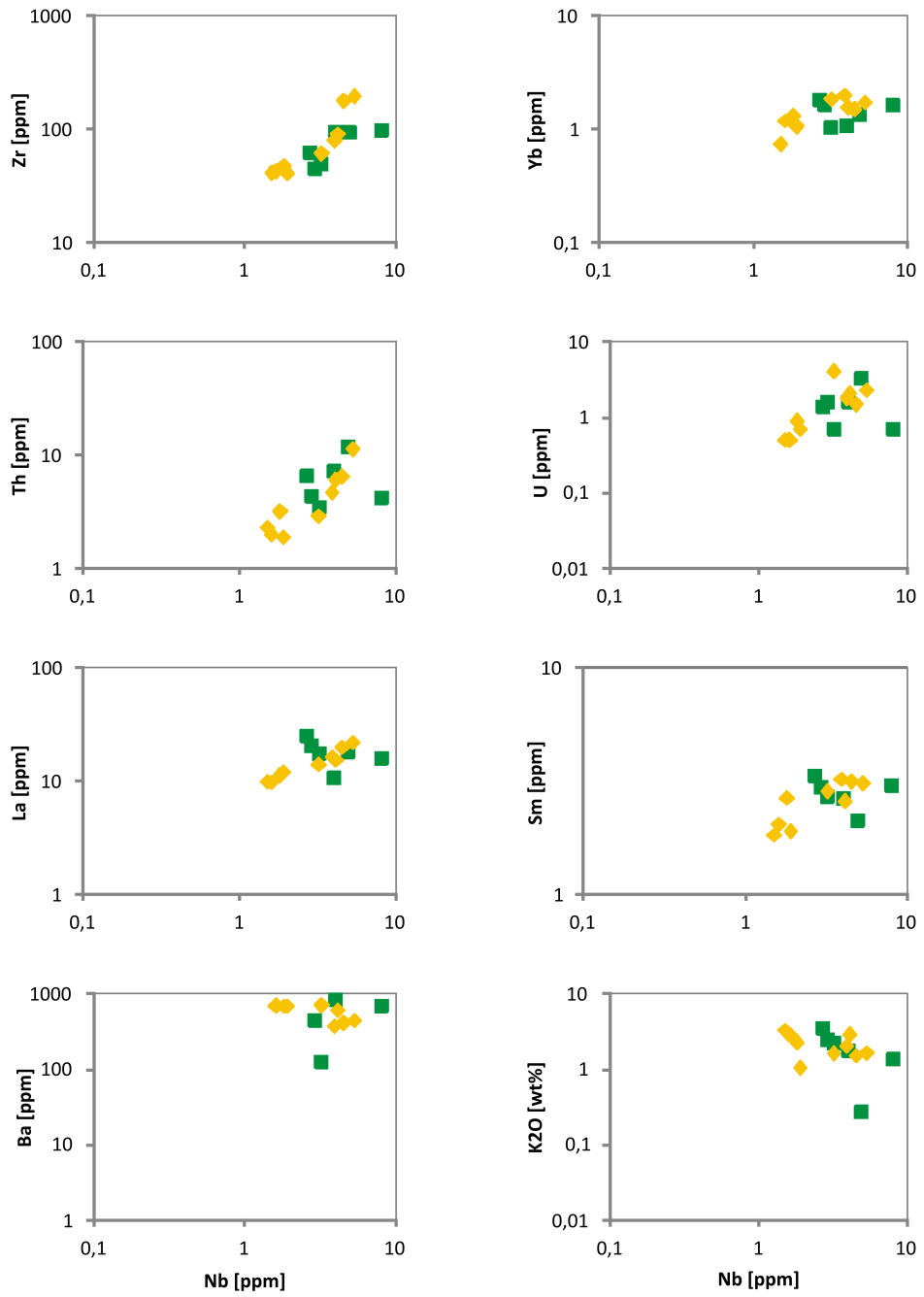


Figure 5.1.: Testing element mobility in samples of the Dereköy (green) and Cambu (yellow) Formation (Cann, 1970)

5.3. Determining the rock type

The most famous rock classification diagrams for identification of volcanic rock types are the alkali versus silica diagrams. [Le Bas et al. \(1986\)](#) and [Middlemost \(1994\)](#) developed TAS diagrams where they plot the acidity on the horizontal axis and alkalinity on the vertical axis. $\text{Na}_2\text{O} + \text{K}_2\text{O}$ is selected to distinguish alkali from sub-alkali rock types and SiO_2 should mirror the transition from primitive to evolved rock types, as SiO_2 is a proxy for the degree of differentiation. For first classification the tuff samples have been plotted in the TAS diagram of [Le Bas et al. \(1986\)](#), (Fig. 5.2). Sample T13/12b/T, T13/38/T and T13/48/T plot on the ultra basic side and show alkaline affinity, like sample T13/30b/T which is classified by the TAS diagram as Trachybasalt and also seems to have more alkaline character. The three last-mentioned seem to be modified in their major element chemistry, as other classifications show. Another sample sticking out is sample T13/42/T, which lies in the dacite field next to the boundary to the rhyolite field. This very acidic composition in contrast is confirmed by immobile element classifications. All the other samples lie in the andesite (T13/34/T, T13/37/T, T13/40/T), basaltic andesite (T13/30a/T, T13/39/T) and basalt field (T13/03/T, T13/12/T, T13/37b/T, T13/38/T). Two samples have too low SiO_2 abundances to be plotted in this diagram. But TAS diagrams are vulnerable to effects of alteration and therefore not the best choice to plot altered volcanic rocks. Immobile elements should be preferred over alteration-affected major elements to classify the rock type.

Floyd and Winchester developed a volcanic rock classification diagram based on trace elements ([Floyd and Winchester, 1975, 1978](#); [Winchester and Floyd, 1976, 1977](#)). It can be also used for altered volcanic rocks, as it uses robust element ratios (Fig. 5.3). The ratio of Nb/Y was assigned as proxy for alkalinity instead of $\text{Na}_2\text{O} + \text{K}_2\text{O}$. From sub-alkali to alkali composition the ratio increases. The proxy is a good one in sodic systems and less reliable in potassic, because Nb represents and magnifies the behavior of Na (Nb is more incompatible). Nb and K are largely decoupled during subduction and therefore correlate less well ([Pearce, 1996](#)). Further Zr/TiO_2 was selected as proxy for silica, higher ratios mirroring increasing acidity. During crystallization of olivine, pyroxene and plagioclase in basalts this ratio changes only little, but it increases when oxides enter the system, Ti gets compatible and Fe-Ti-oxides are formed. The magnitude of the ratio of Zr, which is incompatible

throughout the fractionation and Ti, which becomes compatible during fractional crystallization, is therefore a good indicator of extend of fractionation. Zr/TiO₂ fractionates less in comparison to Nb/Y when garnet is involved (Pearce, 1996). The classification is proposed to be used as a filter for basalt discrimination diagrams such as Ti-Zr-Y (Pearce and Cann, 1973) and Th-Ta-Hf (Wood, 1980). Only data points plotting in the basic, sub-alkaline basalt field (and intermediate alkaline trachyandesite field for Th-Ta-Hf) should be used for basalt classification.

The plot of Winchester and Floyd (1977) was further developed by Pearce (1996), who also addressed some problems of misclassification. Volcanic arc magmas have typically high water content, which polymerizes the melt thus creating oxidizing conditions under which Fe-Ti-oxides crystallize earlier and Si-content increases in the residual melt. This causes a large overlap of island arc basalts, basaltic andesites, andesites and dacites. Moreover, volcanic arc basalts and syn-collision rocks commonly lie in the intermediate area because mantle sources are modified by subduction melts and contain higher ratios of Zr/Ti (Pearce, 1996). So it is possible that originally basic volcanic arc basalts plot in the intermediate field due to a subduction component. After Pearce (1996) the tuff samples classify mainly in the basic, sub-alkaline basalt field, except of six samples of intermediate sub-alkaline andesite to basaltic andesite composition, one of them (T13/42/T) lying on the boundary to dacitic composition (Fig. 5.4). Rhyodacitic to dacitic composition is confirmed for this sample and two further (T13/37/T, T13/40/T) by the plot of Winchester and Floyd (1977), (Fig. 5.3). Two samples (T13/12/T, T13/48/T) are classified as andesites and all other samples plot in the andesite/basalt field.

Hastie et al. (2007) reconstructed the TAS diagram with immobile elements, which behave similar during subduction zone processes, but remain immobile during surface weathering (Fig. 5.5). Robust equivalent proxies for the K₂O-SiO₂ diagram for classifying also intensively altered volcanic arc lavas are used. As a proxy for potassium an immobile element is applied, which becomes mobile during subduction, behaves non-conservative and is transferred from the subducting slab to the mantle wedge. Thorium and cerium are highly incompatible during mantle melting and fractional crystallization at intermediate to acidic compositions, but behave non-conservative and are added to the mantle wedge during subduction (Pearce, 1996). Hastie et al. (2007) went for Th as a proxy for K, as Th mirrors K in terms of immobility perfectly. The only difference is seen in the non-conservative property,

which occurs at different temperatures for different elements. The release of Th is taking place at greater depth than the release of the usual fluid elements like K or Ba (Becker et al., 2000; Savov et al., 2005). Thus at cool subduction setting, in shallow depth it is possible that only K, not Th, is transported by crust-derived fluids. But sediment melt at greater depth will then transport both (Hastie et al., 2007). So partial decoupling during subduction should not be a problem as all parts contribute to magma genesis. Th stands its immobility during weathering and metamorphism up to upper amphibolites facies, whereas K can get mobilized by volcanic fluids circulating and thus be depleted in altered volcanic rocks. Moreover, SiO₂ should be replaced as well by an appropriate proxy. During fractional crystallization and assimilation in most sub-alkaline magmas Si is slightly incompatible. As proxy cobalt, a compatible element is chosen which behaves inverse to silica and is gradually removed from the melt throughout crystallization from basalt to rhyolite. The significant inverse relationship is clearly visible when looking at behavior during fractional crystallization. Co is strongly partitioning into olivine and Fe-Ti oxides, slightly compatible for partitioning in pyroxene and amphibole and strongly incompatible for partitioning in feldspar. Compared to the discrimination diagram of Winchester and Floyd (1977), Co is potentially a better proxy for SiO₂ than the ratio of Zr/TiO₂ as it is neither influenced by oxide, nor zircon saturation in the melt (Hastie et al., 2007). Also during alteration Co behaves inverse to silica, as it stays immobile when Si gets mobile during weathering (e.g. Trescases, 1973). For the development of the Th-Co discrimination diagram Cenozoic to recent island arc samples were used and for testing Cretaceous basic calc-alkaline and intermediate-acid tholeiitic volcanic arc series were used. The biggest overlap for classification of the rock type is stated to be between basalt and basaltic andesite to andesite rock types (Hastie et al., 2007). Two samples plot in the basaltic field, four are classified dacitic/rhyolitic and the rest lies in-between in the basaltic andesite to andesitic array.

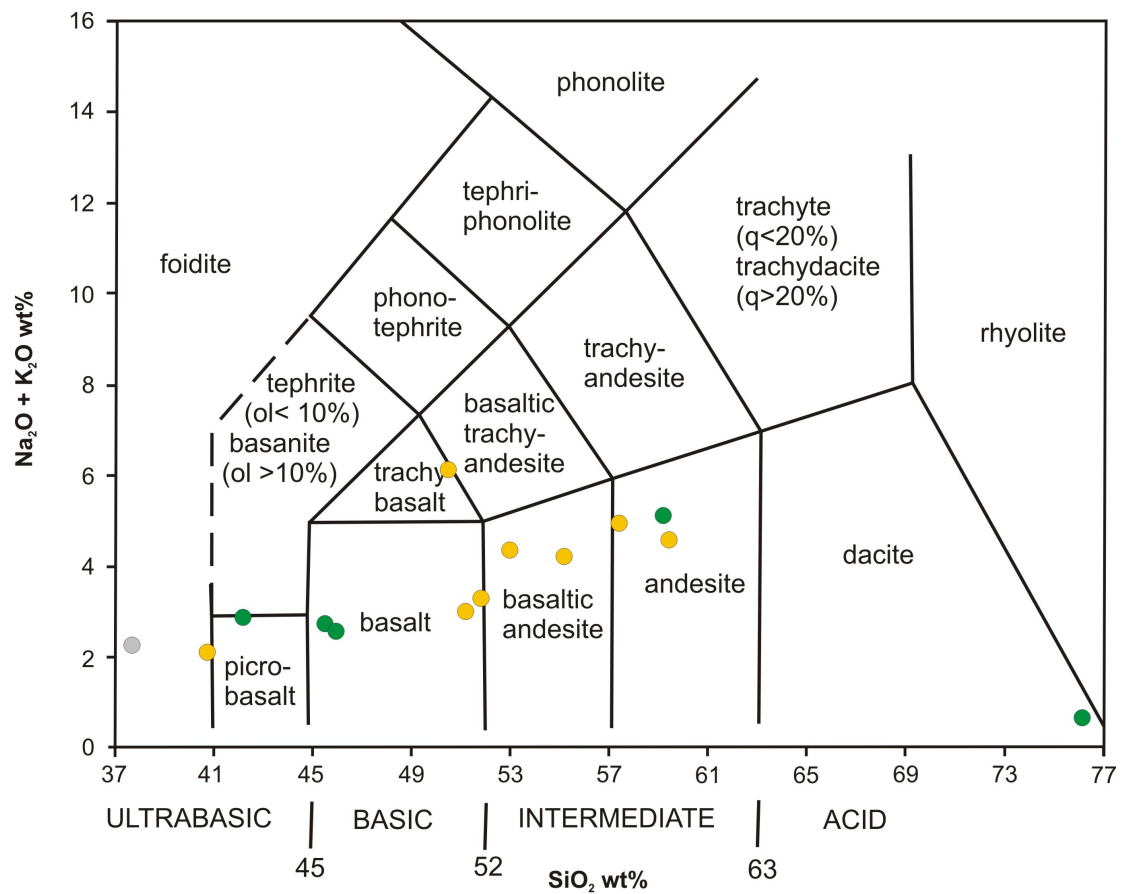


Figure 5.2.: Total alkali versus silica diagram after Le Bas et al. (1986); samples of Dereköy (green), Cambu (yellow) and Akveren (grey) Formation

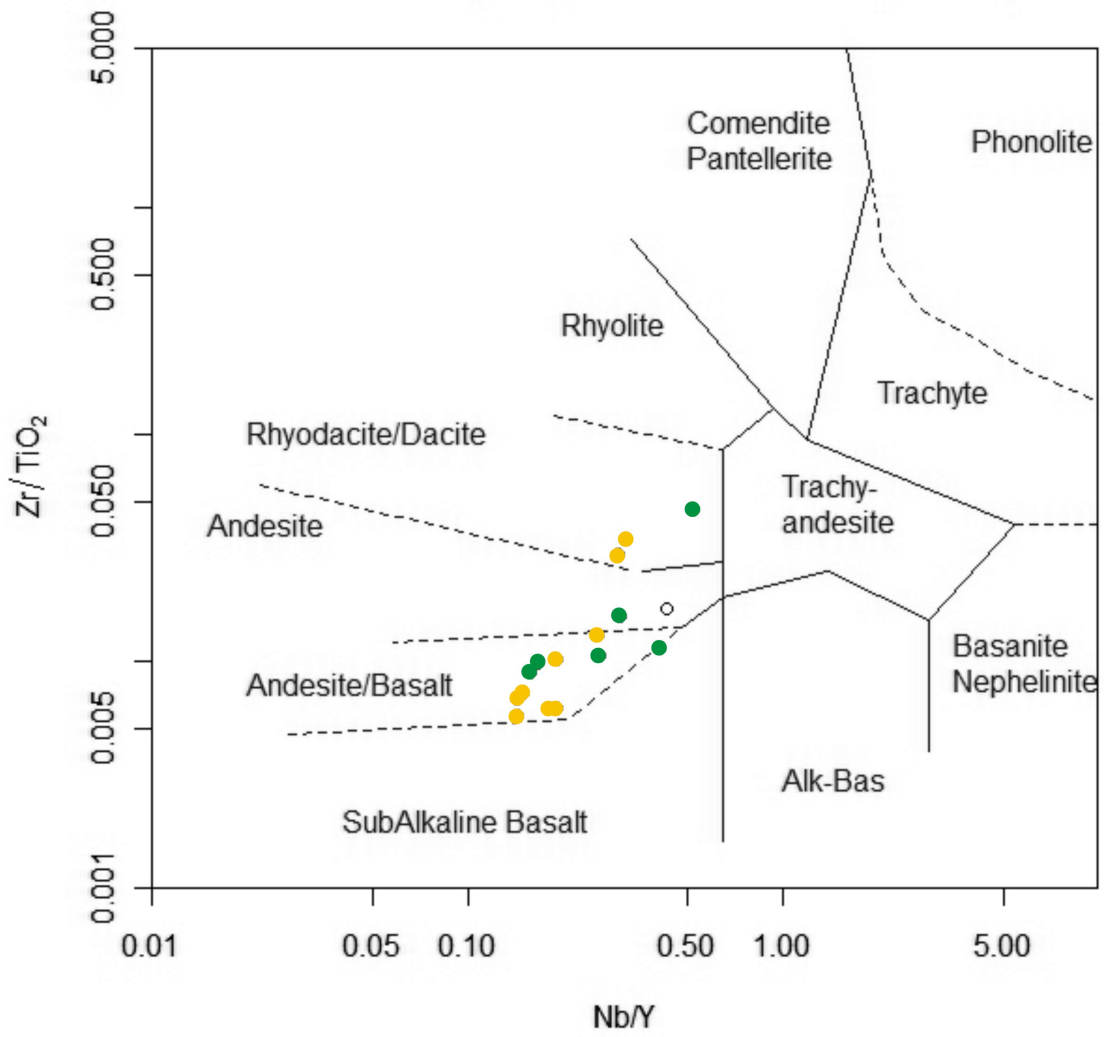


Figure 5.3.: Zr/TiO_2 - Nb/Y discrimination diagram after Winchester and Floyd (1977)

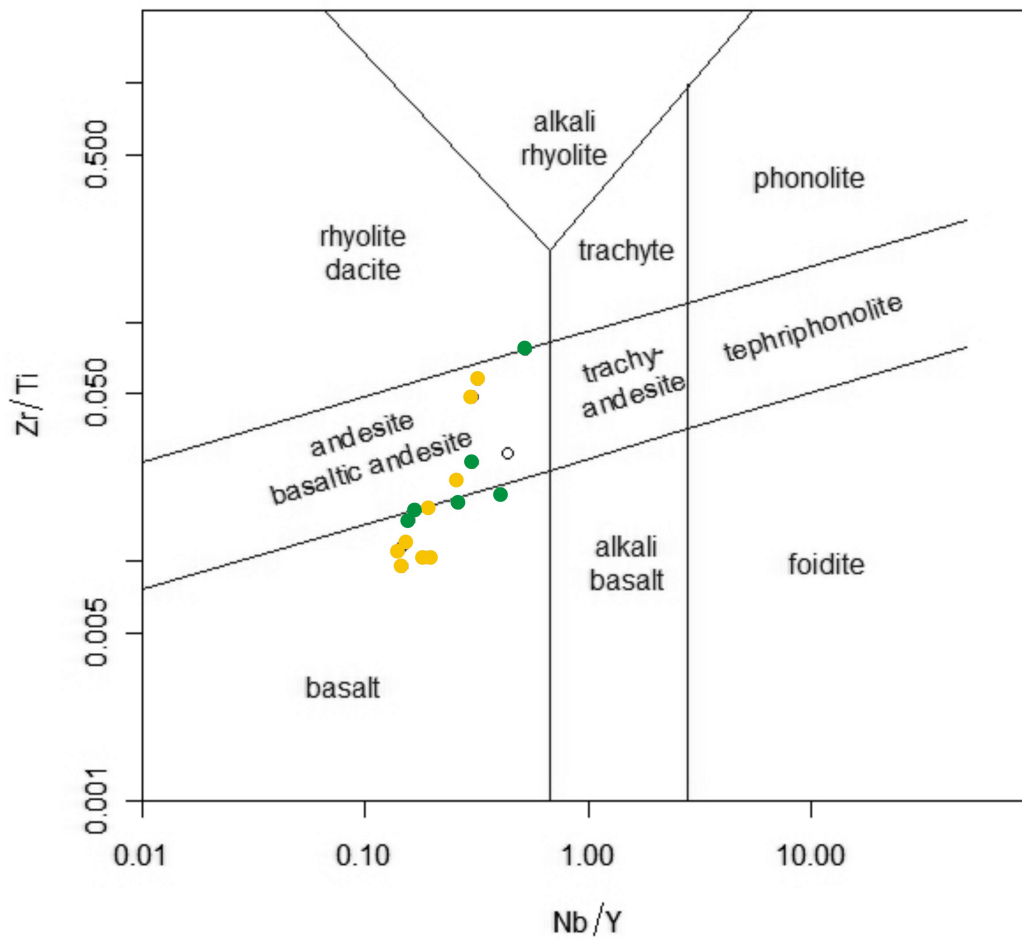


Figure 5.4.: Zr/Ti-Nb/Y discrimination diagram after Pearce (1996)

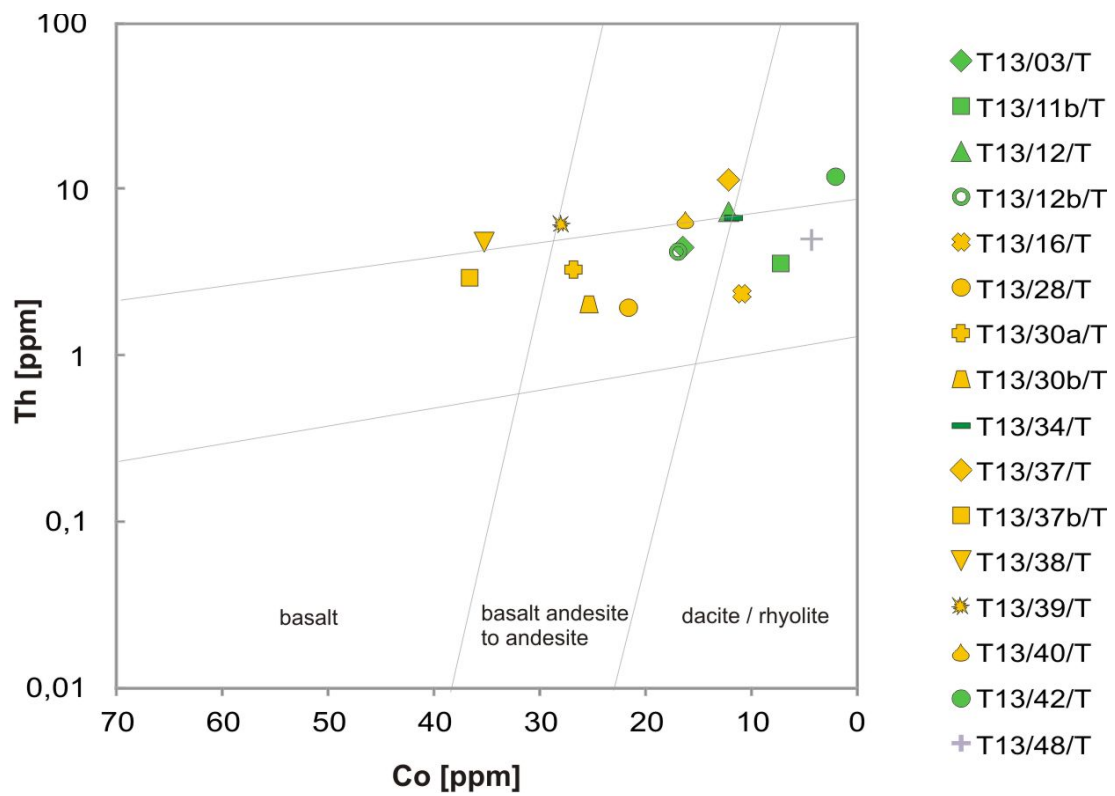


Figure 5.5.: Th-Co discrimination diagram after Hastie et al. (2007)

5.4. Discriminating volcanic series

In the classic TAS diagram of [Le Bas et al. \(1986\)](#) (Fig. 5.2) or the Zr/Ti-Nb/Y diagram of [Winchester and Floyd \(1977\)](#) (Fig. 5.3) the rock type is discriminated, but the volcanic series cannot be distinguished. Whether the series are tholeiitic, calc-alkaline- high K calc-alkaline or shoshonitic can be assigned by looking at the enrichment of large ionic lithophile elements (LILE), hence K_2O for example. So [Peccerillo and Taylor \(1976\)](#) developed a K_2O-SiO_2 diagram classifying into the different volcanic series. In Fig. 5.6 a K_2O-SiO_2 TAS diagram (after [Le Bas et al., 1986](#)) and the [Peccerillo and Taylor \(1976\)](#) diagram where combined. Only one sample is attributed to be tholeiitic dacite in this classification (T13/42/T), two others are calc-alkaline andesites (T13/37/T, T13/40/T), another four are high K calc-alkaline (T13/30a/T, T13/34/T, T13/37b/T, T13/38/T) and all the others are shoshonitic. The comparison of $K_2O+Na_2O-SiO_2$ (Fig. 5.2) and K_2O-SiO_2 TAS diagram (Fig. 5.6) also displays outliers, where Na is explicitly higher than other samples. In three samples the Na_2O numbers are around 3wt%. Sample T13/30b/T is classified as a trachybasalt, but could actually be a basalt, if sodium is modified, whereas andesite classification of sample T13/37/T and T13/40/T stays the same. A further attempt to subdivide the rocks into volcanic series was done by using more immobile elements by [Pearce \(1982\)](#). Non conservative immobile elements, which do not remain in the slab but are transferred to the mantle wedge, will plot above the mid-oceanic ridge basalt (MORB) field (Fig. 5.7). The trace element ratios Th/Yb and Ta/Yb are used to discriminate between Island arc tholeiitic, calc-alkaline and shoshonitic series. As Th is a good proxy for K, the magnitude of ratio Th/Yb is increasing with increasing potassium from tholeiitic to shoshonitic as well and is therefore used as alkalinity index. The trace element ratios are better for the discrimination of volcanic series, than for rock type identification because they are not depending on effects of fractional crystallization in general. The data of the tuff samples shows calc-alkaline to shoshonitic affinity. Nine samples plot in the shoshonitic and six samples in the calc-alkaline field in this projection. Sample T13/30b/T could not be plotted here, because Ta was below the detection limit. Moreover, volcanic series are also identified by the described Th-Co discrimination diagram ([Hastie et al., 2007](#)). The tuff samples plot in the calc alkaline to high-K calc-alkaline range (Fig. 5.8).

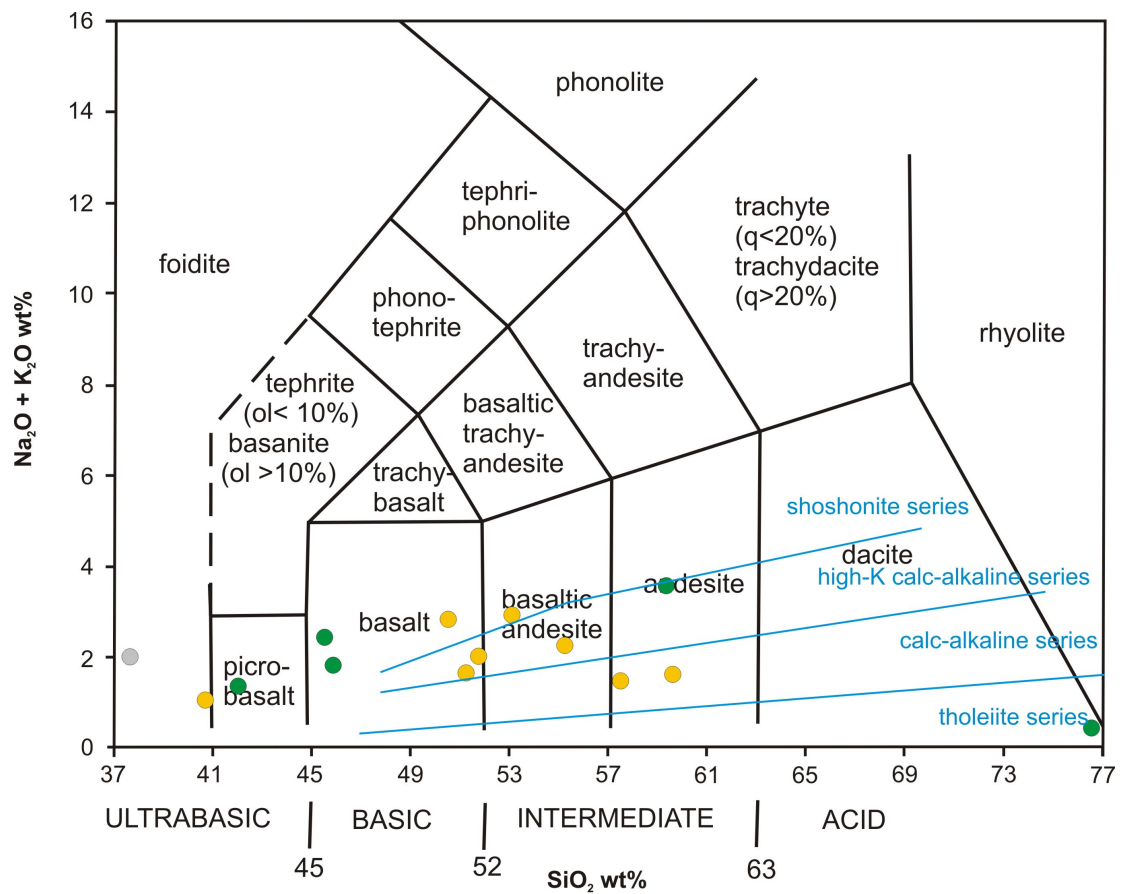


Figure 5.6.: Combined K_2O - SiO_2 TAS diagram after Le Bas et al. (1986) and Pecerillo and Taylor (1976)

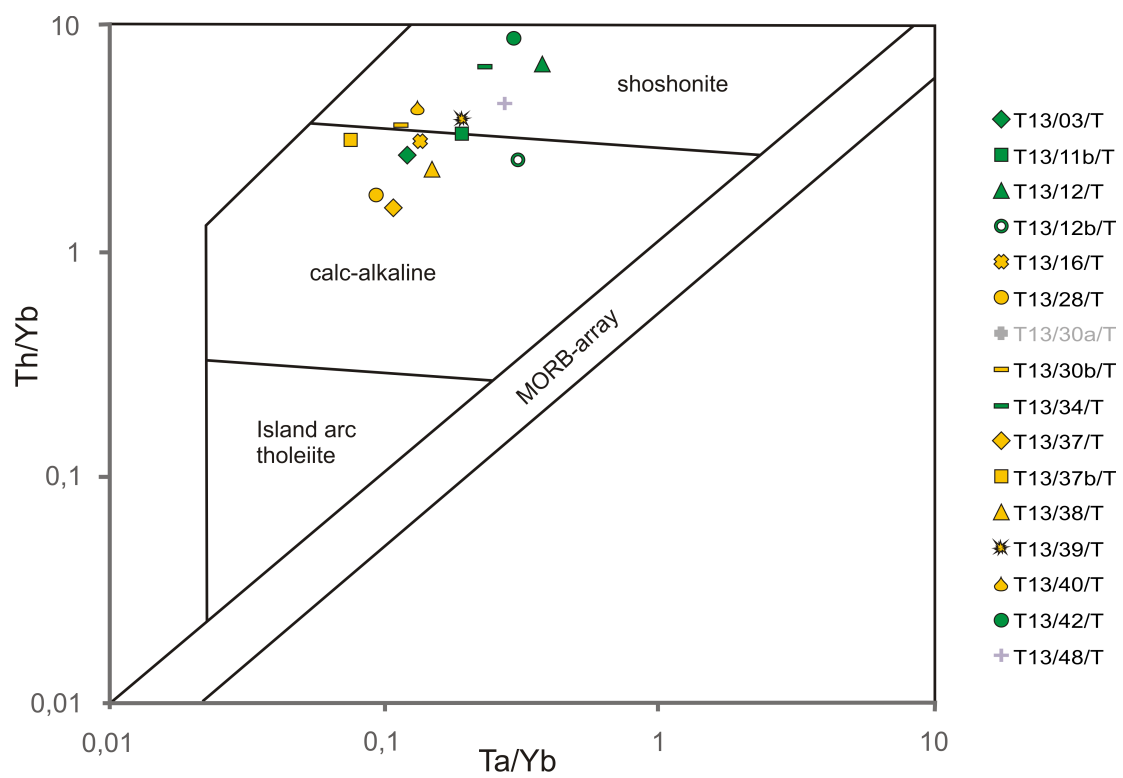


Figure 5.7.: Th/Yb-Ta/Yb diagram after Pearce (1982)

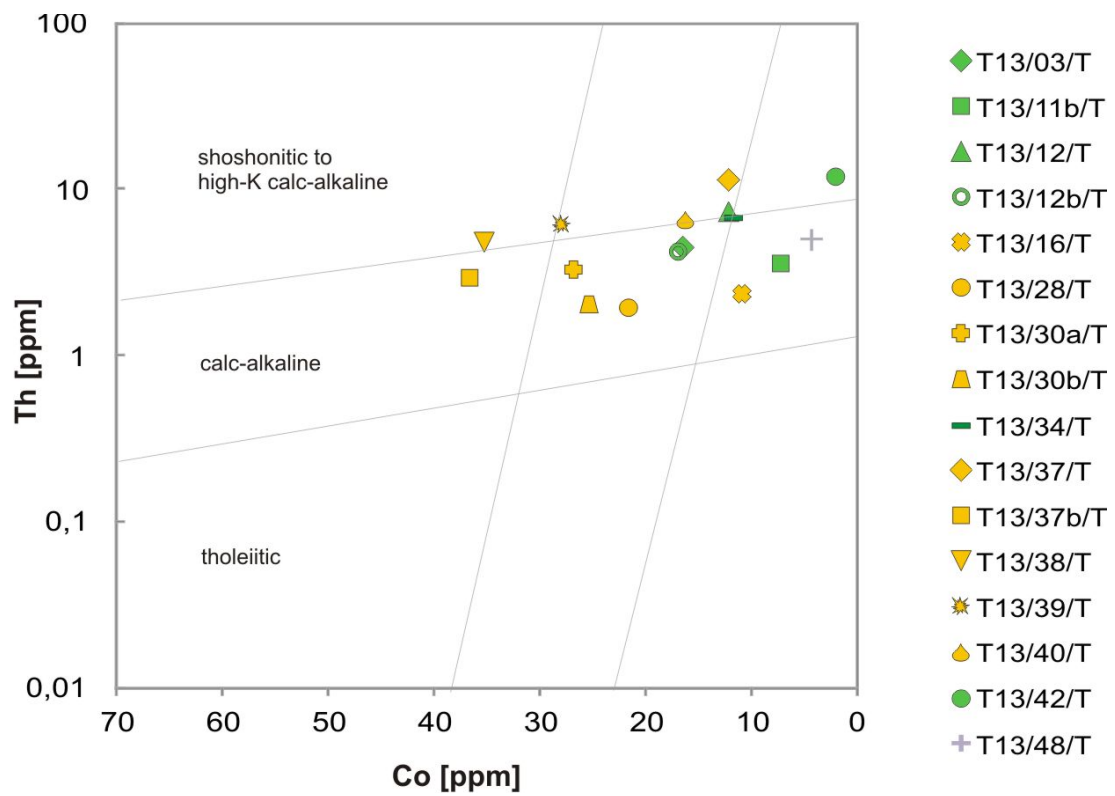


Figure 5.8.: Th-Co discrimination diagram after Hastie et al. (2007)

5.5. Revealing the tectonic setting

Moreover, after rock types and volcanic series have been obtained, different tectonic discrimination diagrams are used. The Ti-Zr-Y diagram from [Pearce and Cann \(1973\)](#), (Fig. 5.9) is a good (95%) indicator for within-plate affinity and excludes latter for all our samples, except one from Alayazi section (T13/16/T). Transitional settings between volcanic arcs and within-plate settings are difficult to handle with this classification. Within-plate basalt (WPB) at attenuated continental crust can plot beyond the boundaries of the WPB field in the calc-alkaline basalt (CAB) or mid-oceanic ridge basalt (MORB) array. Those samples which plot within the MORB/CAB/IAT (island arc tholeiites) transitional field (T13/28/T, T13/30a/T, T13/30b/T, Cayalti section) can with greater confidence be assigned as volcanic arc products, than the more zircon rich CAB samples (T13/11b/T, T13/12/T, T13/12b/T, Kuscu section). The samples, which plot outside the drawn boundaries, could be likely to represent an interaction of magma and upper crust.

Further, the Th-Hf-Ta diagram ([Wood, 1980](#)) was consulted and displays a uniform CAB affinity (Fig. 5.10). The selective enrichment of Th is very typical for volcanic arc basalts in connection with syn-collision magmas and it is enriched in the mantle above subduction zones. The main magma type seems to be of volcanic arc origin, as magmas from transitional VAB/WPB settings would have probably higher content of Ta. But of course eruptions at attenuated continental lithosphere bear very similar signatures like at subduction zones and can also plot in the VAB array. The question is, if Th represents a true subduction component or assimilation of continental crust. To answer this one can consult the Ti/V discrimination diagram of [Shervais \(1982\)](#), (Fig. 5.11). Here about half of the samples plot in the oceanic-floor basalt (OFB) field and therefore seem to originate not from a volcanic arc setting *sensu stricto*, but maybe from a marginal basin close to a subduction zone. But this diagram is very vulnerable as not using element ratios, but only V and Ti values, which can be affected by dilution, cumulative crystallization or alteration to a notable extend. The same has to be considered when applying the discrimination after [Pearce \(1982\)](#) where only Zr and Ti values are looked at (Fig. 5.7). [Pearce and Norry \(1979\)](#) use the Zr/Y ratio for discrimination of the different settings (Fig. 5.12). The investigated samples plot outside the fields for island arc, mid-ocean ridge and within-plate basalts. On one hand this can be an effect of fractional crystallization

as Zr values plotted on the x-axis are not plotted in a ratio and change significantly, like Y does as well, during this process. On the other hand the Zr/Y ratio is not likely to be different at fast or slow spreading ridges. As our samples are plotting on the left side of the supposed fields, having lower Zr values, they have an origin at a slow spreading ridge. A similar classification like with the Zr-Y-Ti diagram from [Pearce and Cann \(1973\)](#) is done by [Meschede \(1986\)](#), using Nb instead of Ti. Acting as an alkalinity indicator, Nb helps to achieve a distinction between normal MORB (N-MORB) and plume-influenced MORB (P-MORB) and points out N-MORB affinity for your samples (Fig. 5.13). Further the great majority of the samples plot in the two fields indicating volcanic arc basalts (C, D). Within-plate basalts should have higher Zr/Y and Nb/Y ratios and volcanic arc origin is confirmed once again. Finally [Agrawal et al. \(2008\)](#) confirms, by using a logarithmic two dimensional plotting of four element ratios of La/Th, Sm/Th, Yb/Th and Nb/Th the elucidated tectonic setting, by classifying all samples as island arc derived basalts (Fig. 5.14).

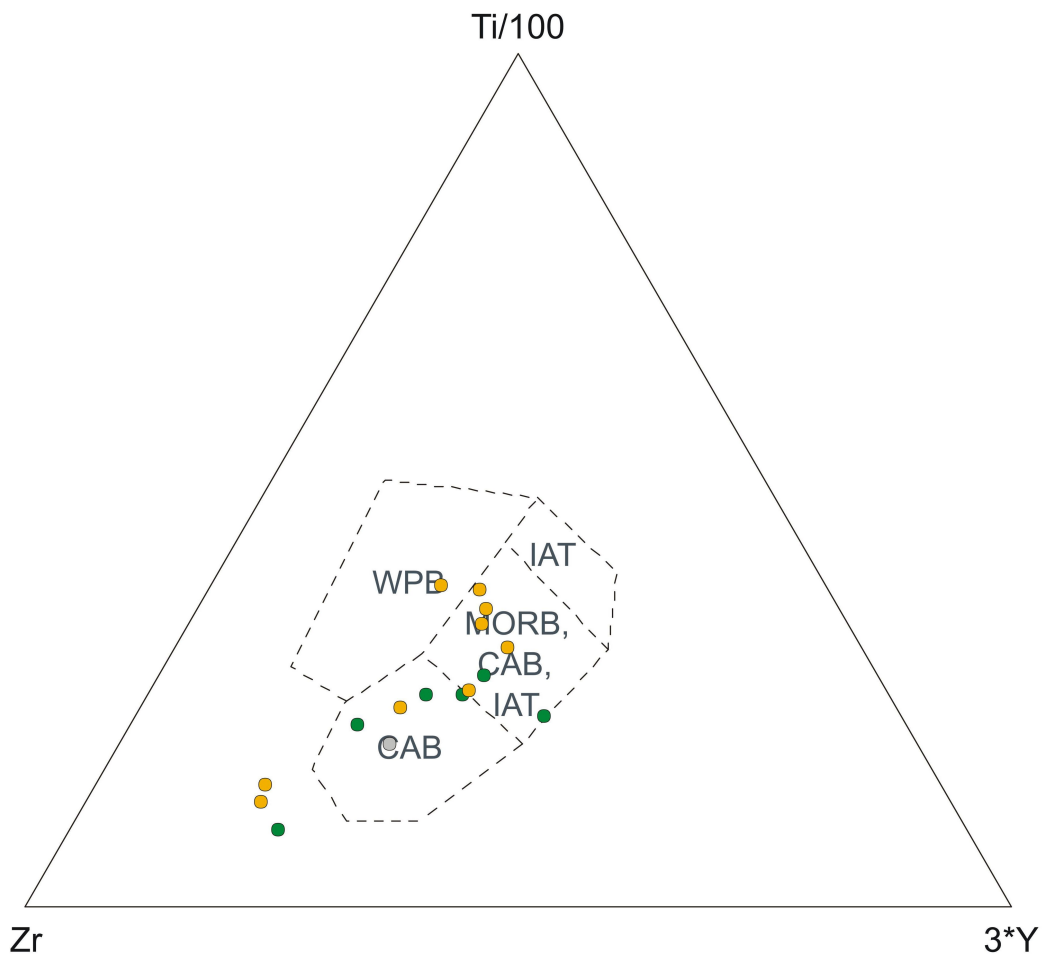


Figure 5.9.: Ti-Y-Zr discrimination diagram after Pearce and Cann (1973)

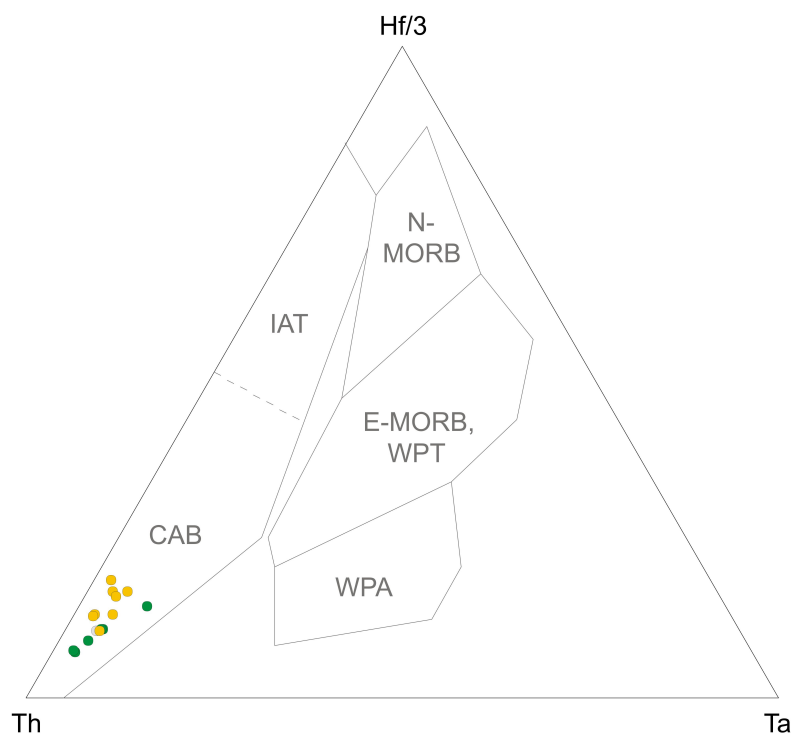


Figure 5.10.: Hf-Ta-Th discrimination diagram after Wood (1980)

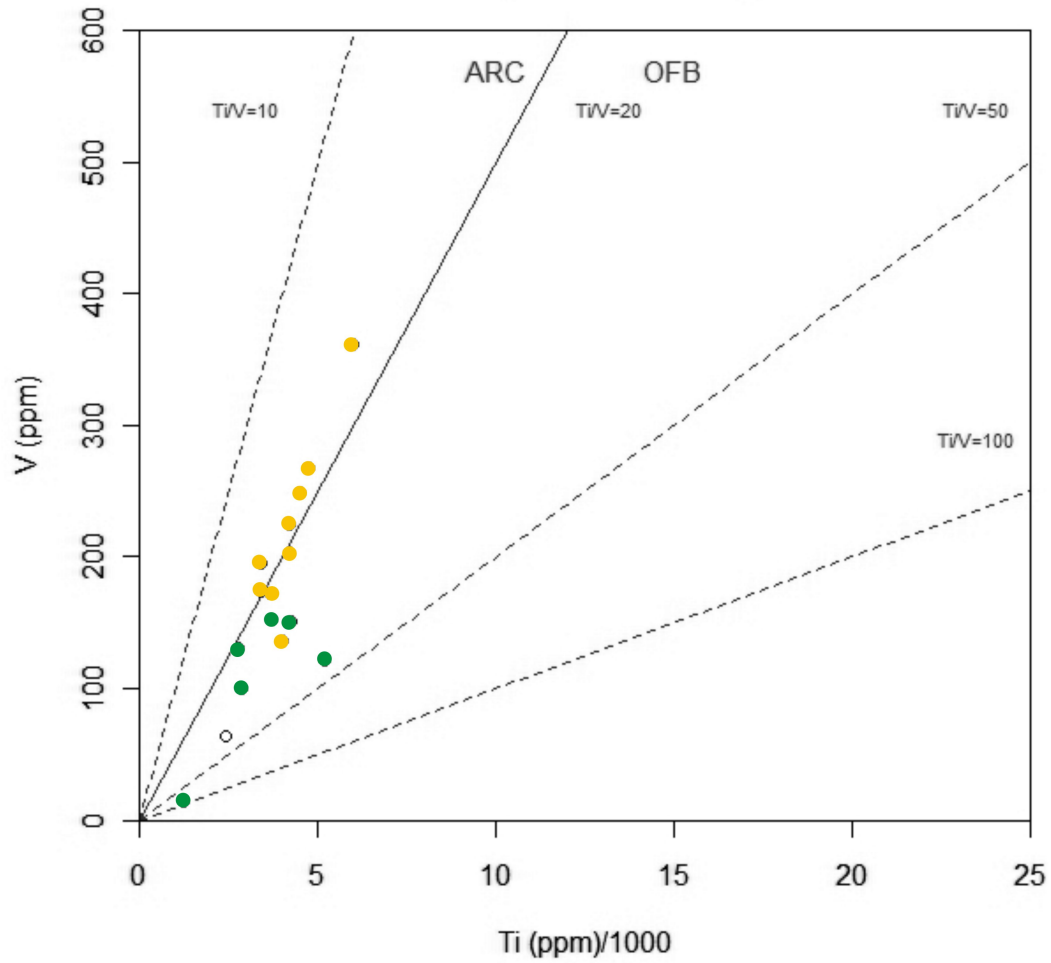


Figure 5.11.: V/Ti discrimination diagram after Shervais(1982)

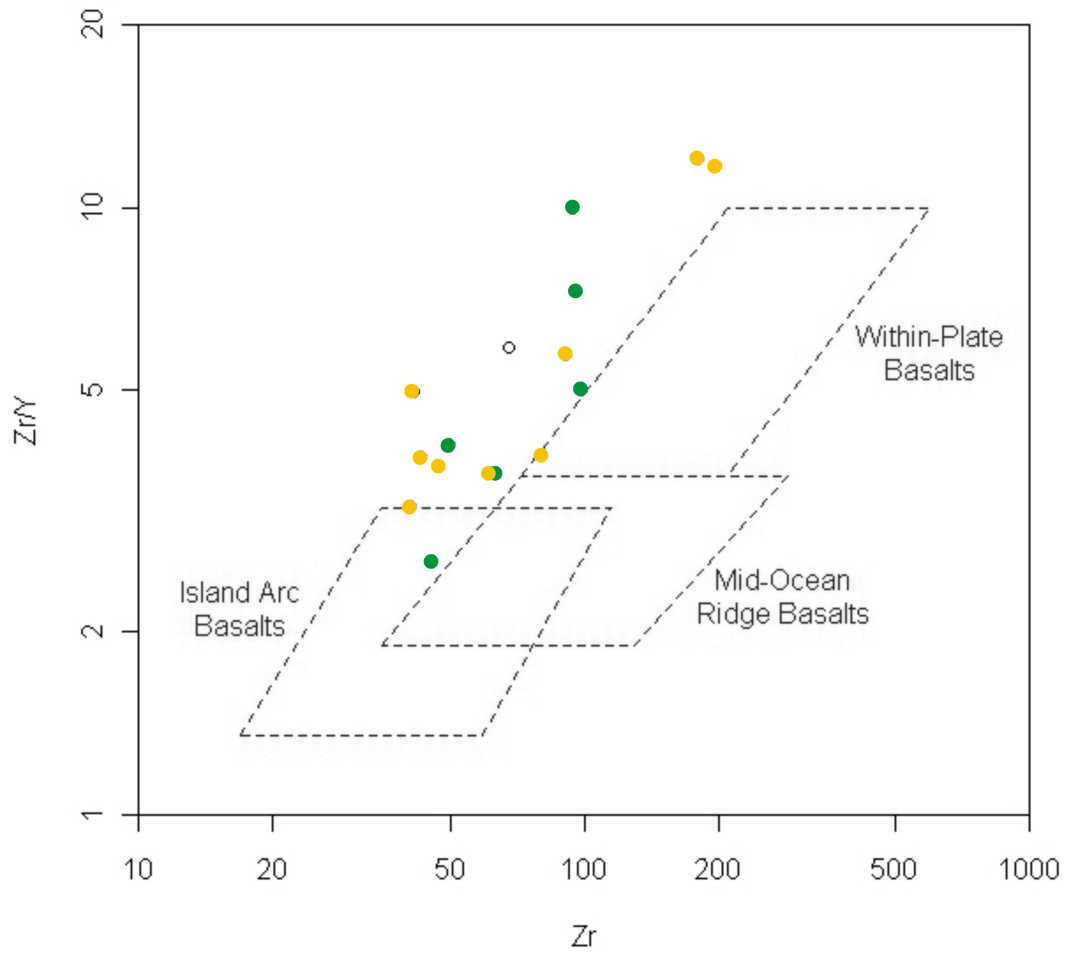


Figure 5.12.: Zr/Y-Zr discrimination diagram after Pearce and Norry (1979)

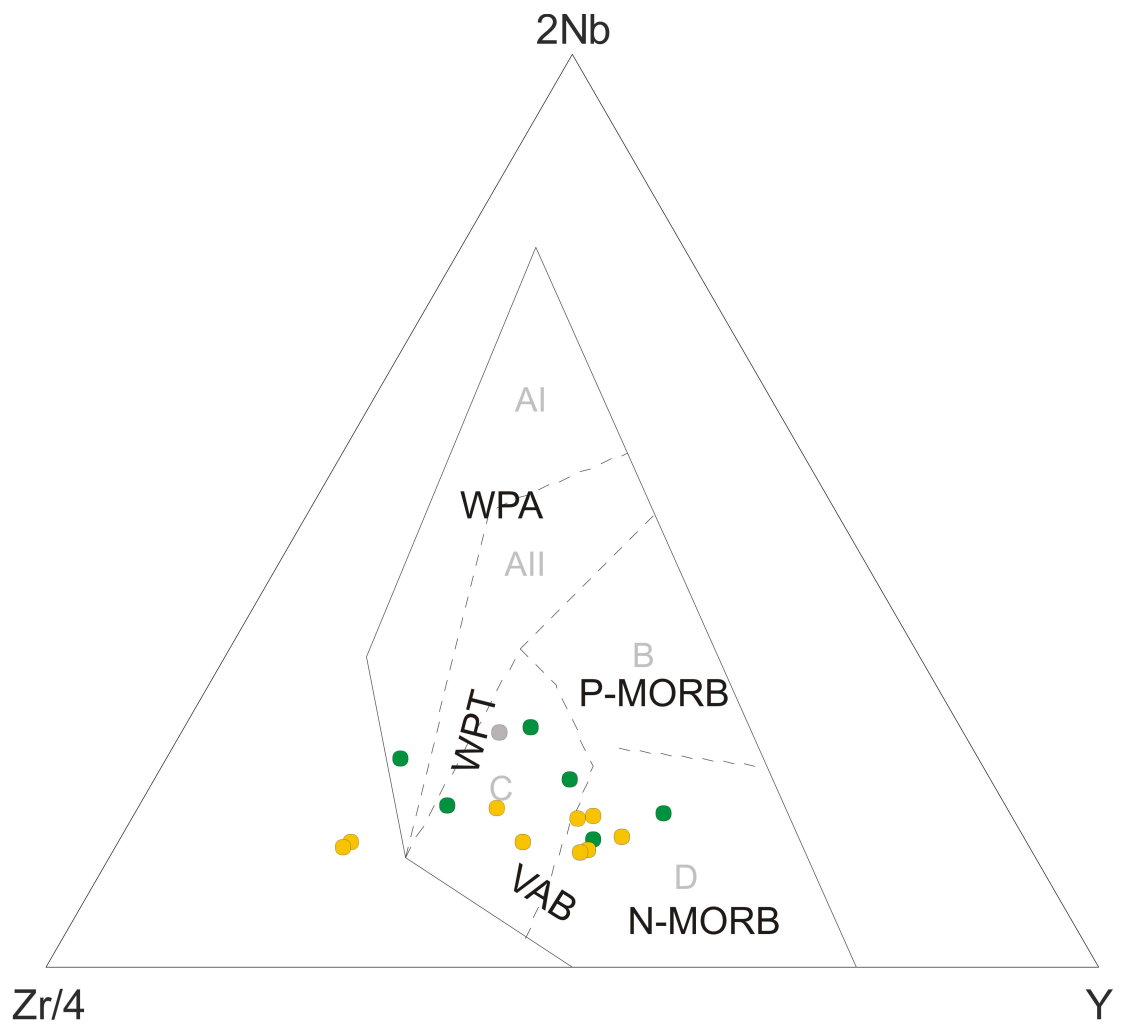


Figure 5.13.: Nb-Y-Zr discrimination diagram after Meschede (1986)

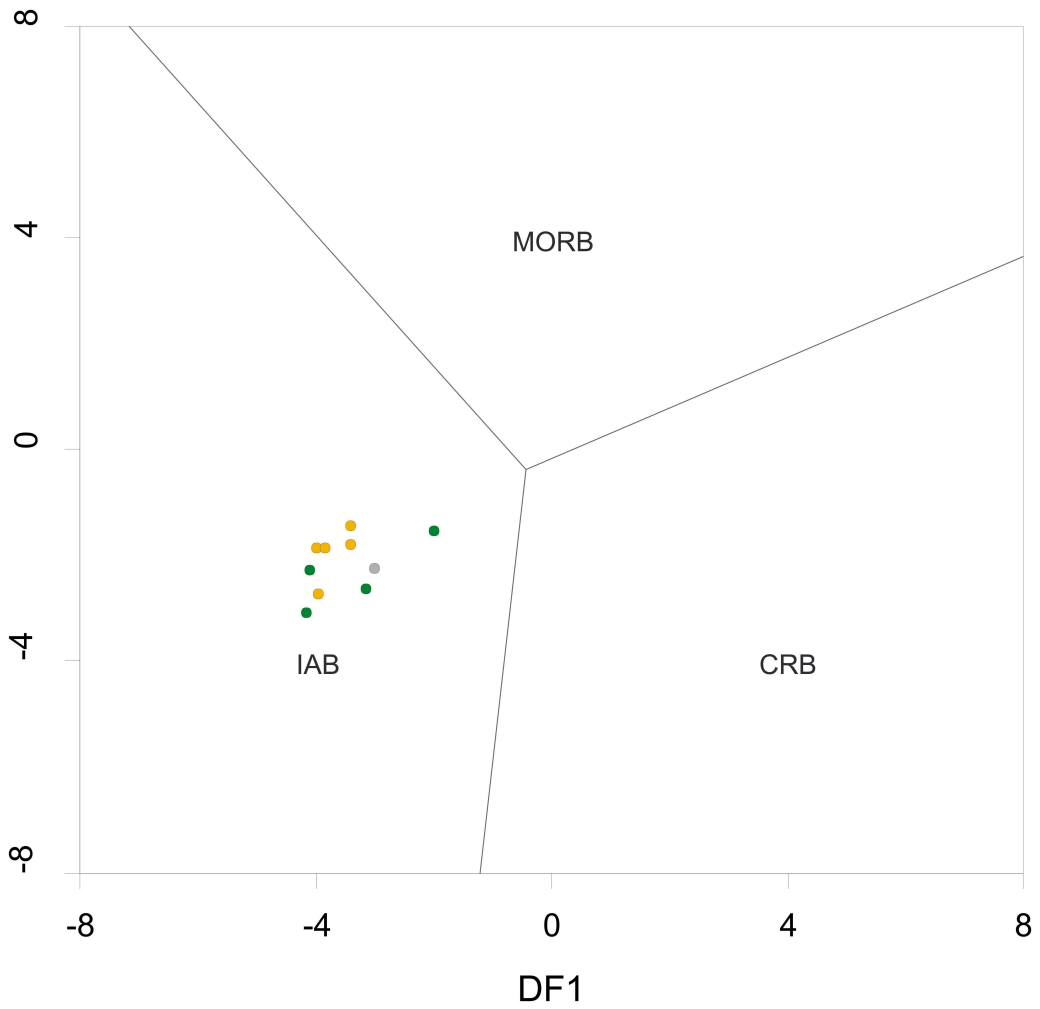


Figure 5.14.: La/Th, Sm/Th, Yb/Th and Nb/Th discrimination diagram after Agrawal et al. (2008)

5.6. Plotting geochemical element patterns

Each rock association has characteristic abundances of trace elements, depletion and enrichment in relation to other elements and normalizing values. There are of course pairs and groups of elements with very similar geochemical properties and behavior. Picking out one representative of each allows powerful discrimination of rock types, volcanic series and tectonic setting after normalizing to N-type MORB. Six elements were chosen, bearing meaningful information on conservative behavior as well as compatibility during mantle melting and fractional crystallization (Pearce, 1996). The plotted element variations are another powerful tool for discriminating volcanic arc rocks (Fig. 5.15). The element patterns show a distinct Nb anomaly, with respect to Th and Ce, which is typical for volcanic arc patterns (Pearce, 1996). While Th and Ce are preferentially transferred to the melting column, Nb stays in the subduction plate, mainly within amphiboles, but also within titanite or rutile and is causes this characteristic depletion. Four samples of Alayazi and Cayalti seem to have a more tholeiitic character, as Nb is depleted with respect to N-type MORB. Further Zr, Ti and Y values lie below those of N-MORB. All other samples are classified as calc-alkaline and high-K calc-alkaline arc basalts. These more alkaline arc basalts are enriched in Nb and Zr relative to N-MORB, whereas Ti and Y are depleted as in the other VAB samples. The two groups of tholeiitic and calc-alkaline arc basalts can be further subdivided into suites ranging from basalts to rhyolites (Pearce, 1996). Moreover, the steepness of the gradient between Th and Nb in the samples correlates well to the VABs classified by of Pearce (1996). Only sample T13/12b/T shows a shallower gradient and slightly increased Nb, Ti and Y in comparison to the other samples. This could be a transition between VAB and WPB following the arguments of Pearce (1996). One sample (T13/42/T) is enriched in Th and shows a more significant negative Ti anomaly than the other samples. This can be interpreted as an effect of increasing fractional crystallization. In a basic magma crystallization of pyroxene, olivine and amphibole do not show any impact on Ti, but as soon as the composition gets more acidic and Ti-bearing oxides like magnetite are fractionated Ti will further deplete. The change in acidity is also displayed when looking at the discrimination diagrams, where sample T13/42/T plots in rhyodacitic compositions and shows shoshonitic character. The Ti /Zr ratio changes conspicuously when magnetite fractionation starts, causing a depletion in Ti and further enrichment of Zr. Further in two samples (T13/37/T,

Multi-element diagram (normalized to N-MORB)

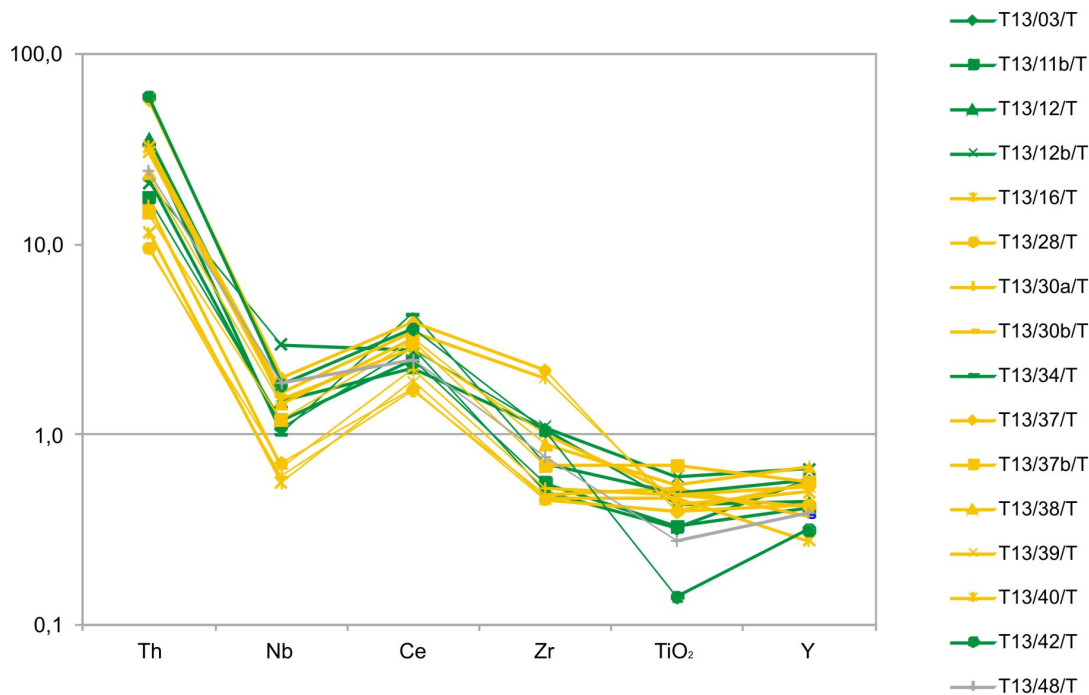


Figure 5.15.: Patterns of selected elements normalized to NMORB after Pearce (1996)

T13/40/T Zr values lie well above those of the others. The increased abundances of Zr in these two samples can be also seen in the discrimination diagrams (Pearce and Cann (1973), Fig. 5.9; Meschede (1986), Fig. 5.13). Zirconium is highly incompatible during mantle melting and fractional crystallization up to intermediate to acidic compositions and behaves conservative. The Zr enrichment could be interpreted as a shift in acidity or depth of melting. Moreover sample T13/40/T shows microscopic abundances of zircon minerals. As not only primary prismatic volcanic zircons are present, but also rounded sedimentary zircons are included, an admixture of older sediment is likely and could explain the zirconium outlier as well. The Zr enrichment causes displacement to higher Zr/TiO₂ ratios and probably to the rhyodacite/dacite field in the discrimination diagram of Winchester and Floyd (1977) (Fig. 5.3). Further exactly those two samples with increased Zr values lie beyond the defined fields in the triangular diagrams of Pearce and Cann (1973) and Meschede (1986).

5.7. Summary of the geochemical classification

Summing up three different rock types discrimination diagrams have been used to classify the tuff samples. All using alkalinity and acidity or proxies of those to compare the samples with the drawn arrays, which are based on classified rocks. TAS diagrams (Le Bas et al., 1986; Middlemost, 1994), Nb/Y-Zr/TiO₂ a more immobile element classification (Winchester and Floyd, 1977; Pearce, 1996) and the Th-Co discrimination diagram (Hastie et al., 2007) assign mainly basalt to basaltic andesite to andesite to rhyodacite types. Further combined (Le Bas et al., 1986; Pecerillo and Taylor, 1976; Hastie et al., 2007) and non-combined (Pearce, 1982) diagrams elucidate volcanic series when the tuffs have been erupted. According to the discrimination diagrams applied an overall trend can be seen in being non-tholeiitic and predominantly calc-alkaline to shoshonitic character. Then the tectonic setting was defined by several discrimination diagrams using immobile elements and element ratios (Pearce and Cann, 1973; Wood, 1980; Meschede, 1986; Agrawal et al., 2008). Within plate setting can be excluded, except for one sample. The more probable scenario is an arc setting; this trend is confirmed by corresponding results. Transitional settings are a bit complicated to handle with those discrimination diagrams, but may anyway only be associated with a minority of samples. Finally the multi-element diagrams refer perfectly to the discrimination diagrams used for gaining information on rock type, volcanic series and tectonic setting, emphasize the afore mentioned results (Table 5.1, Table B.3). According to this summary there are many correlations between the different classification diagrams, but of course there are also outliers and special cases elucidated by different diagrams. This can be ascribed to element mobility of during weathering when using K₂O, Na₂O and SiO₂ or maybe also measuring accuracy in case of Na₂O. Further some element abundances, like Ti, are affected largely by fractional crystallization, which is itself depending on acidity and oxygen fugacity. Variations in abundances of immobile elements sometimes gives arise to additional environmental conditions, like depth of melting, mixing of magma, crustal components or subduction features.

Table 5.1.: Overview of the geochemical classification results

sample T13/.../T	Classification according to							
	Nb/Y-Zr/TiO ₂ (Pearce, 1996)	Th-Co (Hastie et al., 2007)	Th/Yb-Ta/Yb (Pearce, 1982)	Th-Co (Hastie et al., 2007)	Ti-Zr-Y (Pearce and Cann, 1973)	Zr/4-2Nb-Y (Meschede, 1986)	Th-Hf-Ta (Wood, 1980)	La/Th- Sm/Th- Yb-Th-Nb- Th (Agrawal, 2008)
37b	Ba	Ba	c.a.	c.a.	MORB/CAB/IAT	VAB/NMORB	CAB /VAB	Island Arc Basalt
38	Ba	Ba	c.a.	c.a.	MORB/CAB/IAT	VAB/NMORB	CAB /VAB	Island Arc Basalt
28	Ba	BaAnd-And	c.a.	c.a.	MORB/CAB/IAT	VAB/NMORB	CAB /VAB	Island Arc Basalt
30a	Ba	BaAnd-And	c.a.	c.a.	MORB/CAB/IAT	VAB/NMORB	CAB /VAB	Island Arc Basalt
30b	Ba	BaAnd-And	(Ta below detection limit)	c.a.	MORB/CAB/IAT	VAB/NMORB	CAB /VAB	Island Arc Basalt
03	Ba	BaAnd-And	c.a.	c.a.	MORB/CAB/IAT	VAB/NMORB	CAB /VAB	Island Arc Basalt
34	Ba	BaAnd-And	shos	c.a. - h.k	MORB/CAB/IAT	VAB/NMORB	CAB /VAB	Island Arc Basalt
12b	Ba	BaAnd-And	c.a.	c.a.	CAB	VAB	CAB /VAB	Island Arc Basalt
12	And-BaAnd	BaAnd-And	shos	c.a. - h.k	CAB	VAB	CAB /VAB	Island Arc Basalt
39	And-BaAnd	BaAnd-And	shos	c.a.	CAB	VAB	CAB /VAB	Island Arc Basalt
40	And-BaAnd	BaAnd-And	shos	c.a. - h.k	-	-	CAB /VAB	Island Arc Basalt
37	And-BaAnd	BaAnd-And	shos	h.k. - shos	-	-	CAB /VAB	Island Arc Basalt
11b	Ba	DaRy	shos	c.a.	CAB	VAB	CAB /VAB	Island Arc Basalt
48	And-BaAnd	DaRy	shos	c.a.	CAB	VAB	CAB /VAB	Island Arc Basalt
16	Ba	DaRy	shos	c.a.	WPB	VAB	CAB /VAB	Island Arc Basalt
42	DaRy	DaRy	shos	h.k.- shos	-	WPA	CAB /VAB	Island Arc Basalt

6. Discussion

The first part of this discussion is going to deal with the question whether two different volcanic formations can be distinguished with the results of geochemistry. Further the characteristics of the Lower and Upper Volcanic Succession in the investigated area are going to be described. The second part is going to compare the results of this study with results from literature. The next part is then going to point towards the paleogeographic discussion again, asking the question about the characteristics of the volcanic arc.

6.1. Correlation of geochemistry interpretation with the two volcanic formations

According to the selection of sampled spots by the possibility of correlation of tuffs with biostratigraphy, the number of samples is limited and the interpretation of the geochemistry does not show distinctive groups. An assignment to different formations would therefore not be non-ambiguous without the correlation to relative ages. Using this age information obtained through biostratigraphy, a characterization of the two volcanic formations based on the geochemical interpretation, is possible. Furthermore, a correlation makes sense as two volcanic units are described in literature and be compared then.

Following all samples in this study, assigned to Dereköy Formation, have a basaltic to andesitic composition. Only [Hastie et al. \(2007\)](#) classifies the sample T13/11b/T as dacite/rhyolite. But according to the primary data used for developing this diagram, there is quite a big overlap between basaltic andesite/andesite and dacite/rhyolite field. Moreover the samples are calc-alkaline to high-K calc-alkaline and shoshonitic. Further the tectonic setting is an arc setting according to all classification diagrams

used. Sample T13/42/T is excluded from these general statements. This sample is significantly more acidic in composition and plots in the dacite /rhyolite range within all diagrams.

The samples belonging to the Cambu Formation are also classified as basalts to basaltic andesites to andesites. Two samples (T13/37/T and T13/40/T) seem to be a bit more acidic plotting in the dacite/rhyolite field in the diagram of [Winchester and Floyd \(1977\)](#). In agreement with statements from the literature, volcanic series include a slightly more tholeiitic trend within the uniform volcanic arc origin. The classification diagrams ([Peccerillo and Taylor, 1976](#); [Pearce, 1982](#); [Hastie et al., 2007](#)) only show a range from calc-alkaline to shoshonitic. However, plotted in the Multi-element-diagram, four element patterns (normalized to N-MORB) show a more tholeiitic volcanic arc character. Samples of Cambu Formation are depleted in Zr, Th and Nb with respect to samples of Dereköy Formation. Further, the presence of a magmatic arc between Turonian and Campanian can be stated on base of this correlation.

6.2. Geochemical studies on volcanics in northern Turkey

Although, the volcanics of the Late Cretaceous can be crucial for understanding of some major paleotectonic discussions including subduction of Neotethys subduction and opening of the Black Sea, there are not as many geochemical publications in this interesting area, as one would think. However, there are some and so the question arises if the results of this study fit the descriptions in literature.

Different volcanic formations are distinguished in the Upper Cretaceous alongside the Black Sea coast. In the Western and Central Pontides the two volcanic successions are the Turonian-early Santonian Dereköy Formation and the Campanian Cambu Formation ([Tüysüz et al., 2012](#)).

The Dereköy Formation is thought to be deposited contemporaneously with the rifting in the Western Black Sea basin. Calc-alkaline and acidic to intermediate lavas and pyroclastics, bearing subduction signature and produced by a depleted

mantle are described by [Tüysüz et al. \(2012\)](#). The volcanic sequence starts with basalt andesitic composition and evolves towards dacitic and rhyodacitic with time. This fits to the results of the present work, although despite of a limited sample number it is not possible to confirm this evolution with time.

Similar to the Dereköy Formation, the rocks of the Cambu formation are also characterized as amphibole bearing material derived from a mantle source. But further within the Cambu Formation also characteristics of within plate volcanism are mentioned, which imply thinning of the lithosphere and upwelling of the asthenosphere. The volcanic series of the Upper Volcanic Unit are tholeiitic to calc-alkaline, as well as typical within-plate high-K calc-alkaline to shoshonitic. Like in the Lower also in the Upper Volcanic Succession a transition from basalts to andesites to biotite-bearing rhyolite/rhyodacites can be observed ([Tüysüz et al., 2012](#); [Eyüboğlu et al., 2011b](#)). As already mentioned especially the tholeiitic trend can be confirmed by the recent results.

Apart from [Tüysüz et al. \(2012\)](#), there are some additional works from the Western and Central Pontides. [Keskin et al. \(2003\)](#) worked on Late Cretaceous basaltic andesite/andesite/dacite rocks from the area north of Istanbul and confirms a volcanic arc setting. [Cinku et al. \(2009\)](#) did a combined rock magnetic and geochemical study on a broad range of Late Cretaceous volcanic rocks and [Şahin et al. \(2012\)](#) published a study on a Late Cretaceous granodiorite from a calc-alkaline series. Furthermore, there are several studies on volcanics in the Eastern Pontides. Especially [Eyüboğlu et al. \(2011b\)](#); [Eyüboğlu \(2010\)](#) did a lot of geochemical work on Late Cretaceous high-K calc-alkaline to shoshonitic andesites. Latter are classified to have been produced in a continental arc setting ([Eyüboğlu, 2010](#)). Moreover, [Sipahi et al. \(2014\)](#) published a paper on volcanic rocks from Murgul (Eastern Pontides). The results fit very well to other Late Cretaceous volcanics. The rock types range from basalt to rhyolite, the volcanic series are dominantly tholeiitic and an island arc setting is confirmed as well. Also [Bektaş et al. \(1999\)](#) did a study on Late Cretaceous tholeiitic to high-K calc-alkaline andesites from the Eastern Pontides and suggested magma generation at an island arc or back arc.

After the Late Cretaceous younger periods of volcanism developed and several works on Paleogene and Neogene volcanic in northern Turkey can be found in literature. In the Kastamonu area [Peccerillo and Taylor \(1976\)](#) classified Eocene calc-alkaline (basaltic) andesites. [Unal et al. \(2012\)](#) described Miocene vulcanites

around Susurluk, in northwest Turkey. According to classifications they range from medium to high-K calc-alkaline andesites to h-K calc-alkaline dacites and developed from subduction related arc magmas or post collision lavas. Also [Keskin et al. \(2008\)](#) did investigations on middle Eocene volcanic units south of Sinop, which comprise calc-alkaline basalts to rhyolites derived from a magmatic arc. Around Gümüşhane, in the Eastern Pontides [Aslan \(2010\)](#) did a geochemical characterization of arc derived tuffs. The rock types range from basalts to andesites to trachyandesites to rhyolites and the volcanic series are described as tholeiitic, calc-alkaline and shoshonitic. Further in the Eastern Pontides Eocene calc-alkaline basaltic andesites to trachy dacites from a post coalitional setting are described by [Kaygusuz et al. \(2011\)](#) and [Aydin et al. \(2008\)](#) published a paper on Pliocene alkaline basanites to tephrites and basalt.

The geochemical characterizations on volcanics in the Pontides in the Late Cretaceous till the Neogene found in literature are not differing significantly. The existence of a magmatic arc is confirmed by a great majority. The described Late Cretaceous volcanic rock types lie between basaltic to rhyolitic and the volcanic series are shoshonitic, high-K calc alkaline, calc-alkaline to tholeiitic. So the general characterization is in agreement with the recent results.

6.3. Situation of the magmatic arc within the paleogeographic discussion

As described there is a quite broad consensus on an arc setting in the Late Cretaceous in literature (e.g. [Keskin et al., 2008](#); [Tüysüz, 2011](#); [Sipahi et al., 2014](#); [Nikishin et al., 2013](#)) and also present geochemical results point out a clear volcanic arc origin trend of the sampled tuffs. The question is, how does the derivation of the tuff samples from a magmatic arc fit in the Late Cretaceous paleotectonic discussion. Maybe the results can already strengthen or weaken arguments concerning subducting polarity of Neotethys. As there are numerous described occurrences of volcanics, it is probably that the volcanic arc was situated north of the Pontides. More difficult is the decision if the associated subduction zone was dipping north or south. The present geochemical study can neither exclude one or the other. In literature there is understandably a big discussion on the subduction polarity, which

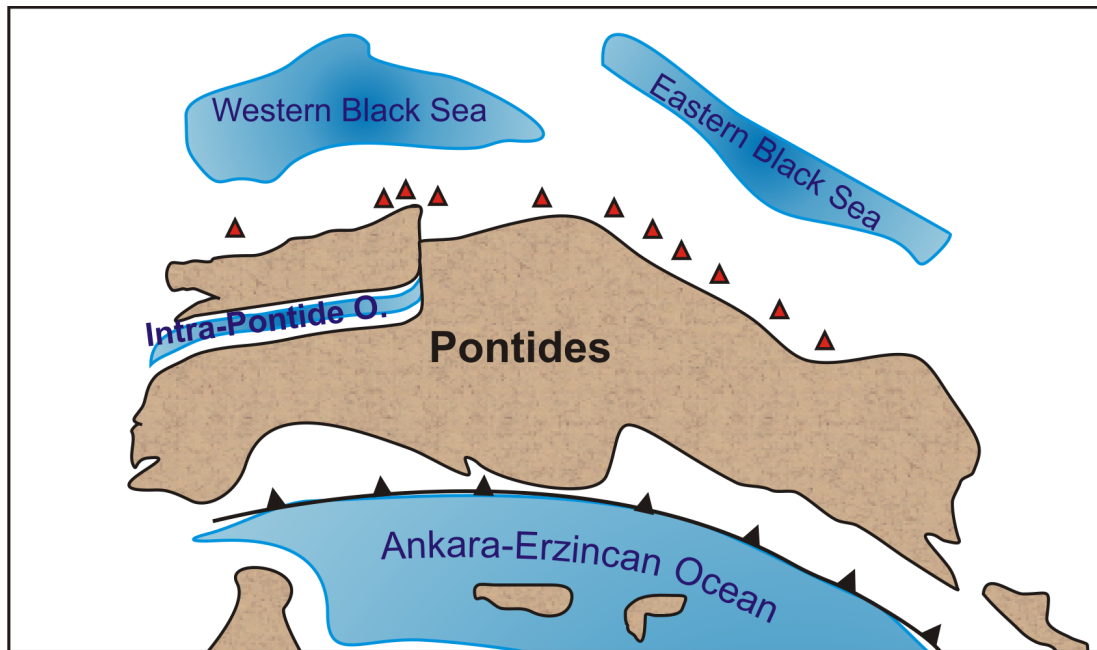


Figure 6.1.: Interpretation of the paleogeography in the Late Cretaceous - subducting Neotethys and volcanic arc, modified from Blakey

is question of principle in Late Cretaceous paleotectonics. As described in previous chapters the northward subduction of Neotethys since Late Cretaceous is a sound model, explaining back arc extension, southward drifting of Istanbul terrane, extension structures on the northern margin of the Pontides and the opening of the Black Sea basin. The arguments for a southward subduction polarity given by [Eyüboğlu et al. \(2011b\)](#) are mainly based on geochemical north-south trends in the Eastern Pontides and a regional-scale south-dipping reverse fault. To solve this controversy discovery of similar and reliable trends in the Western Pontides, as well as the rating of extension structures and reverse faults will be necessary. However, a better characterization of the Pontide magmatic arc could bring new insights. Till then the magmatic arc in the paleotectonic sketch will rest on a white area (Fig. 6.1). What did the northern margin of the Pontides look like and how rapid and steep was the transition to the western Black Sea basin? Was a shelf developed there? Or did the extension structures favor a rather “steep coast”. Is it possible to have tholeiitic magmas as well, despite being in minority, if the arc was delivered by a northward subducting oceanic plate?

7. Outlook

As this geochemical study on Upper Cretaceous tuffs seems to link complex and not yet understood reconstructions of paleogeographic and paleotectonic development of the Neotethys in the Late Cretaceous, further steps revealing the Campanian evolution of Neotethys in Turkey are of great interest. A correlation of the volcanoclastics from the Western Pontides, with those from the Eastern Pontides or even from the Mudurnu-Göynük area could be a big step towards the exposure of overall development of the arc igneous activity. The development of the arc volcanism is multifarious and obviously cannot be covered entirely by the investigation of a limited amount of tuff samples. Desirable further geochemical works can take up those promising results and proceed. The Neotethys evolutions, as well as the one from the Black Sea basin, are oceanographic questions not only important for understanding geology of Turkey but the global (Neotethys) development in the Late Cretaceous. The arc volcanism is a promising link in understanding. Of course the stratigraphic reconstruction and correlation with biostratigraphy would be enhanced by the presence of absolute ages. However, mineral dating is not an easy task to fulfill with those altered Late Cretaceous tuff samples. Zircons were rare in the investigated samples. Only one sampled outcrop shows promising notable higher amounts in zircon minerals, suggestions to revisit the section and find a good biostratigraphic correlation make sense there. Moreover, dating of amphiboles may be very useful to correlate to absolute ages, although they will not be as high in accuracy as zircon ages for sure. A further promising step would be the measurement of isotopes (Sr, Rb, Nd) for improvement of characterization of magma origin.

8. Conclusio

With the investigation of geochemistry of Upper Cretaceous tuffs from the southwestern Black Sea coast and the correlation of latter with biostratigraphic results, the volcanism of Dereköy and Cambu Formation was further characterized. Moreover changes in paleoenvironment and paleotectonic settings in the Neotethyan realm were further revealed by the characterization of the volcanoclastics. As working on Upper Cretaceous altered tuffs, the element mobility was important to be taken into account, when doing interpretations based on element abundances and relations. By a large range of well selected discrimination diagrams the tectonic setting and origin of the samples was confirmed as volcanic arc setting. Further the rock types determined range from basalts to andesites to rhyodacites in both volcanic successions respectively. The volcanic series could be roughly constrained to be dominantly calc-alkaline to shoshonitic, and less often tholeiitic. In addition the correlation with relative ages and developments gained from biostratigraphy allows the allocation to the two volcanic cycles in Late Cretaceous and consequently a rough geochemical characterization of the cycles. Latter reveals, according to the tuffs sampled within this study, less alkalinity and acidity for the Cambu Formation with respect to Dereköy Formation. The paleotectonic position of the determined volcanic arc reinforces discussions about the northern margin of the Pontides, Black sea development and not yet clearly solved subduction polarity of the branched Neotethys.

9. Acknowledgements

Finally I would like to thank my supervisor Michael Wagreich for his support. He gave me the feeling to have placed his trust in me doing this sort of exotic geochemical work within the (bio-)stratigraphically focused project. Further I wish to thank Ismail Yilmaz and Okan Tüysüz for their competent explanations during the field trips and the regional expertise shared during email conversations. Moreover I am very thankful to Susanne Gier and Erik Wolfgring for their support. Many thanks also to Sabine Hruby-Nichtenberger for assistance in laboratory work and Claudia Beybel for preparation of thin sections.

List of Figures

1.1. Outcrops visited in the Western Pontides	11
1.2. Paleogeographic map of the branched Neotethys in the Late Cretaceous, modified from Blakey	13
1.3. Insert of major geologic units (white), suture zones (turquoise) and faults (red) of Turkey in a Google Earth Image	14
1.4. Geologic map of Turkey, modified from Stampfli, 1998; Moix, 2008; Okay and Tüysüz, 1999	15
1.5. Tectonic interpretation of the Turkey-Black Sea area, attention to Western and Eastern Black Sea basin, N-S trending Western Black Sea and West Crimean Fault (red), arrangement of the Pontides	19
1.6. Sedimentary basins in the Western and Central Pontides, modified from Tüysüz (2011)	21
1.7. Occurrence of middle to Late Cretaceous volcanism. Modified from Dewey et al., 1973	22
1.8. Stratigraphy: Cambu and Dereköy Formation, sampled units are marked with *, modified from Tüysüz, 2011	24
4.1. Powder X-Ray diffractograms of the tuff samples from the Dereköy (green), Cambu (yellow) and Akveren (grey) Formation	32
4.2. Selected photomicrographs of the thin sections of volcanoclastic rocks from the SW Black Sea coast. (a) Vitric fragments (white) with glass inclusions; lithic fragments; carbonate minerals. (b) Lithic fragments, basalt clast with plagioclase and clinopyroxene crystals. (c) Large plagioclase phenocrysts; olivine (greenish); mica; lithic clasts. (d) Altered not-orientated feldspar crystals dominating. (e) Large mica aggregates (brown); fractured feldspars (bigger ones elongated); glass. (f) carbonate cement.	35

5.1. Testing element mobility in samples of the Dereköy (green) and Cambu (yellow) Formation (Cann, 1970)	40
5.2. Total alkali versus silica diagram after Le Bas et al. (1986); samples of Dereköy (green), Cambu (yellow) and Akveren (grey) Formation	44
5.3. Zr/TiO ₂ -Nb/Y discrimination diagram after Winchester and Floyd (1977)	45
5.4. Zr/Ti-Nb/Y discrimination diagram after Pearce (1996)	46
5.5. Th-Co discrimination diagram after Hastie et al. (2007)	47
5.6. Combined K ₂ O-SiO ₂ TAS diagram after Le Bas et al. (1986) and Peccerillo and Taylor (1976)	49
5.7. Th/Yb-Ta/Yb diagram after Pearce (1982)	50
5.8. Th-Co discrimination diagram after Hastie et al. (2007)	51
5.9. Ti-Y-Zr discrimination diagram after Pearce and Cann (1973)	54
5.10. Hf-Ta-Th discrimination diagram after Wood (1980)	55
5.11. V/Ti discrimination diagram after Shervais(1982)	56
5.12. Zr/Y-Zr discrimination diagram after Pearce and Norry (1979)	57
5.13. Nb-Y-Zr discrimination diagram after Meschede (1986)	58
5.14. La/Th, Sm/Th, Yb/Th and Nb/Th discrimination diagram after Agrawal et al. (2008)	59
5.15. Patterns of selected elements normalized to NMORB after Pearce (1996)	61
6.1. Interpretation of the paleogeography in the Late Cretaceous - subducting Neotethys and volcanic arc, modified from Blakey	68

List of Tables

1.1. Overview of sampled formations	26
5.1. Overview of the geochemical classification results	63
A.1. Abbreviations used in the text and/or figures	87
B.1. Coordinates of the outcrops visited alongside the SW Black Sea coast	89
B.2. Geochemical data delivered by AcmeLab Canada	90
B.3. Overview of geochemical classification results	91

Bibliography

- Adamia, S., Gamkrelidze, I., Zakariadze, G., and Lordkipanidze, M. (1974). Adjara-Trialeti trough and the problem of the Black Sea origin. *Geotectonika*, 1:78–94.
- Agrawal, S., Guevara, M., and Verma, S. P. (2008). Tectonic discrimination of basic and ultrabasic volcanic rocks through log-transformed ratios of immobile trace elements. *International Geology Review*, 50(12):1057–1079.
- Armijo, R., Meyer, B., Hubert, A., and Barka, A. (1999). Westward propagation of the North Anatolian fault into the northern Aegean: Timing and kinematics. *Geology*, 27(3):267–270.
- Aslan, Z. (2010). U–Pb zircon SHRIMP age, geochemical and petrographical characteristics of tuffs within calc-alkaline Eocene volcanics around Gümüşhane (NE Turkey), Eastern Pontides. *Neues Jahrbuch für Mineralogie-Abhandlungen: Journal of Mineralogy and Geochemistry*, 187(3):329–346.
- Aydin, F., Karsli, O., and Chen, B. (2008). Petrogenesis of the Neogene alkaline volcanics with implications for post-collisional lithospheric thinning of the Eastern Pontides, NE Turkey. *Lithos*, 104(1):249–266.
- Barka, A. (1992). The North Anatolian fault zone. In *Annales tectonicae*, volume 6, pages 164–195.
- Becker, H., Jochum, K. P., and Carlson, R. W. (2000). Trace element fractionation during dehydration of eclogites from high-pressure terranes and the implications for element fluxes in subduction zones. *Chemical Geology*, 163(1):65–99.
- Bektaş, O., Şen, C., Atici, Y., and Köprübaşı, N. (1999). Migration of the Upper Cretaceous subduction-related volcanism towards the back-arc basin of the eastern Pontide magmatic arc (NE Turkey). *Geological Journal*, 34(1-2):95–106.

- Bozkurt, E. and Mittweide, S. K. (2001). Introduction to the geology of Turkey: A synthesis. *International Geology Review*, 43(7):578–594.
- Büchl, A. and Gier, S. (2003). Petrogenesis and alteration of tuffs associated with continental flood basalts from Putorana, northern Siberia. *Geological magazine*, 140(06):649–659.
- Cann, J. (1970). Rb, Sr, Y, Zr and Nb in some ocean floor basaltic rocks. *Earth and Planetary Science Letters*, 10(1):7–11.
- Chamley, H. (1989). *Clay Sedimentology*. Springer-Verlag, Berlin. 623p.
- Chorowicz, J., Dhont, D., and Adıyaman, Ö. (1998). Black Sea Pontid relationship: interpretation in terms of subduction. In *Third International Turkish Geology Symposium, Ankara, Turkey*, page 258.
- Chorowicz, J., Dhont, D., and Gündoğdu, N. (1999). Neotectonics in the eastern North Anatolian fault region (Turkey) advocates crustal extension: mapping from SAR ERS imagery and Digital Elevation Model. *Journal of Structural Geology*, 21(5):511–532.
- Cinku, M. C., Rammlmair, D., Hisarlı, M. Z., and Orbay, N. (2009). A combined rock magnetic and geochemical investigation of Upper Cretaceous volcanic rocks in the Pontides, Turkey. *Studia Geophysica et Geodaetica*, 53(4):475–494.
- Çoğulu, E. (1975). Petrologic and geochronologic studies in the Gümüşhane-Rize region. *Istanbul Technical University Publication* 112p.
- Dewey, J. and Şengör, A. C. (1979). Aegean and surrounding regions: complex multiplate and continuum tectonics in a convergent zone. *Geological Society of America Bulletin*, 90(1):84–92.
- Dewey, J. F., Pitman, W. C., Ryan, W. B., and Bonnin, J. (1973). Plate tectonics and the evolution of the Alpine system. *Geological society of America bulletin*, 84(10):3137–3180.
- Eyüboğlu, Y. (2010). Late Cretaceous high-K volcanism in the eastern pontide orogenic belt: Implications for the geodynamic evolution of ne turkey. *International Geology Review*, 52(2-3):142–186.

- Eyüboğlu, Y., Bektas, O., and Pul, D. (2007). Mid-Cretaceous olistostromal ophiolitic melange developed in the back-arc basin of the eastern Pontide magmatic arc, northeast Turkey. *International Geology Review*, 49(12):1103–1126.
- Eyüboğlu, Y., Bektas, O., Seren, A., Maden, N., Özer, R., and Jacoby, W. R. (2006). Three-directional extensional deformation and formation of the Liassic rift basins in the Eastern Pontides (NE Turkey). *Geologica Carpathica*, 57(5):337–346.
- Eyüboğlu, Y., Chung, S.-L., Santosh, M., Dudas, F. O., and Akaryalı, E. (2011a). Transition from shoshonitic to adakitic magmatism in the Eastern Pontides, NE Turkey: implications for slab window melting. *Gondwana Research*, 19(2):413–429.
- Eyüboğlu, Y., Santosh, M., Bektas, O., and Ayhan, S. (2011b). Arc magmatism as a window to plate kinematics and subduction polarity: Example from the Eastern Pontides belt, NE Turkey. *Geoscience Frontiers*, 2(1):49–56.
- Finetti, I., Bricchi, G., Del Ben, A., Pipan, M., and Xuan, Z. (1988). Geophysical study of the Black Sea area. *Boll. Geofis. Teor. Appl.*, 30:197–234.
- Fisher, R. V. (1961). Proposed classification of volcanoclastic sediments and rocks. *Geological Society of America Bulletin*, 72(9):1409–1414.
- Fisher, R. V. (1966). Rocks composed of volcanic fragments and their classification. *Earth-Science Reviews*, 1(4):287–298.
- Fisher, R. V. (1984). Submarine volcanoclastic rocks. *Geological Society, London, Special Publications*, 16(1):5–27.
- Fisher, R. V. and Schmincke, H.-U. (1984). *Pyroclastic rocks*, volume 90. Springer Berlin etc.
- Floyd, P. and Winchester, J. (1975). Magma type and tectonic setting discrimination using immobile elements. *Earth and Planetary science letters*, 27(2):211–218.
- Floyd, P. and Winchester, J. (1978). Identification and discrimination of altered and metamorphosed volcanic rocks using immobile elements. *Chemical Geology*, 21(3):291–306.
- Garfunkel, Z. (2004). Origin of the Eastern Mediterranean basin: A reevaluation. *Tectonophysics*, 391(1):11–34.

- Görür, N. (1988). Timing of opening of the Black Sea basin. *Tectonophysics*, 147(3):247–262.
- Görür, N., Cagatay, M. N., Sakinc, M., Sümengen, M., Sentürk, K., Yaltirak, C., and Tchapylyga, A. (1997). Origin of the Sea of Marmara as deduced from Neogene to Quaternary paleogeographic evolution of its frame. *International Geology Review*, 39(4):342–352.
- Gouveia, M., Prudencio, M., Figueiredo, M., Pereira, L., Waerenborgh, J., Morgado, I., Pena, T., and Lopes, A. (1993). Behavior of REE and other trace and major elements during weathering of granitic rocks, Evora, Portugal. *Chemical Geology*, 107(3):293–296.
- Haas, W. (1968). Das Alt-Paläozoikum von Bithynien (Nordwest Türkei). *Neues Jahrbuch für Geologie und Paläontologie, Abhandlungen*, 131:178–242.
- Hastie, A. R., Kerr, A. C., Pearce, J. A., and Mitchell, S. (2007). Classification of altered volcanic island arc rocks using immobile trace elements: development of the Th–Co discrimination diagram. *Journal of Petrology*, 48(12):2341–2357.
- Hempton, M. R. (1987). Constraints on Arabian plate motion and extensional history of the Red Sea. *Tectonics*, 6(6):687–705.
- Hippolyte, J.-C., Müller, C., Kaymakci, N., and Sangu, E. (2010). Dating of the Black Sea basin: New nanoplankton ages from its inverted margin in the Central Pontides (Turkey). *Geological Society, London, Special Publications*, 340(1):113–136.
- Hsü, K. J., Nachev, I. K., and Vuchev, V. T. (1977). Geologic evolution of Bulgaria in light of plate tectonics. *Tectonophysics*, 40(3):245–256.
- Hu, X., Jansa, L., Wang, C., Sarti, M., Bak, K., Wagreich, M., Michalik, J., and Sotak, J. (2005). Upper Cretaceous oceanic red beds (CORBs) in the Tethys: Occurrences, lithofacies, age, and environments. *Cretaceous Research*, 26(1):3–20.
- Hubert-Ferrari, A., Armijo, R., King, G., Meyer, B., and Barka, A. (2002). Morphology, displacement, and slip rates along the North Anatolian fault, Turkey. *Journal of Geophysical Research: Solid Earth (1978–2012)*, 107(B10):ETG–9.

- Hubert-Ferrari, A., King, G., van der Woerd, J., Villa, I., Altunel, E., and Armijo, R. (2009). Long-term evolution of the North Anatolian fault: New constraints from its eastern termination. *Geological Society, London, Special Publications*, 311(1):133–154.
- Karacık, Z. and Tüysüz, O. (2010). Petrogenesis of the Late Cretaceous Demirköy igneous complex in the NW Turkey: implications for magma genesis in the Strandja zone. *Lithos*, 114(3):369–384.
- Kaygusuz, A., Arslan, M., Siebel, W., and Şen, C. (2011). Geochemical and Sr-Nd isotopic characteristics of post-collisional calc-alkaline volcanics in the Eastern Pontides (NE Turkey). *Turkish Journal of Earth Sciences*, 20(1):137–159.
- Keskin, M., Genç, Ş. C., and Tüysüz, O. (2008). Petrology and geochemistry of post-collisional middle Eocene volcanic units in north-central Turkey: evidence for magma generation by slab breakoff following the closure of the northern Neotethys Ocean. *Lithos*, 104(1):267–305.
- Keskin, M., Ustaömer, T., and Yenyol, M. (2003). Stratigraphy, petrology and tectonic setting of Upper Cretaceous volcano-sedimentary units, north of Istanbul, Turkey. In *Symposium the Geology of Istanbul, Chamber of Geological Engineers of Turkey, Kadir Has University, Istanbul*, pages 23–35.
- Ketin, İ. (1966). Anadolu nun tektonik birlikleri. *MTA Dergisi*, 66:20–34.
- Koçyigit, A. (1991). An example of an accretionary forearc basin from northern central Anatolia and its implications for the history of subduction of Neotethys in Turkey. *Geological Society of America Bulletin*, 103(1):22–36.
- Koçyigit, A. (1996). Superimposed basins and their relations to the recent strike-slip fault zone: A case study of the Refahiye superimposed basin adjacent to the North Anatolian transform fault, northeastern Turkey. *International Geology Review*, 38(8):701–713.
- Köksal, S. and Göncüoğlu, M. (1997). Geology of the Idis-Dağı--Avanos area (Nevşehir--Central Anatolia). *Bull. Miner. Res. Explor*, 119:41–58.
- Köksal, S., Göncüoğlu, M. C., and Floyd, P. A. (2001). Extrusive members of post-collisional A-type magmatism in Central Anatolia: Karahidir volcanics, Idis Dağı-Avanos area, Turkey. *International Geology Review*, 43(8):683–694.

- Le Bas, M. J., Le Maitre, R., Streckeisen, A., Zanettin, B., et al. (1986). A chemical classification of volcanic rocks based on the total alkali-silica diagram. *Journal of petrology*, 27(3):745–750.
- Letouzey, J., Biju-Duval, B., Dorkel, A., Gonnard, R., Kristchev, K., Montadert, L., and Sungurlu, O. (1977). The Black Sea: a marginal basin; geophysical and geological data. In *International Symposium on the Structural History of the Mediterranean Basins*, pages 363–376. Editions Technip Paris.
- Manetti, P., Boccaletti, M., and Peccerillo, A. (1988). The Black Sea: Remnant of a marginal basin behind the Srednogorie-Pontides island arc system during Upper Cretaceous-Eocene time. *Bolletino di Geofisica Teorica ed Applicata*, 30:39–51.
- Mann, P. (2007). Global catalogue, classification and tectonic origins of restraining- and releasing bends on active and ancient strike-slip fault systems. *Geological Society, London, Special Publications*, 290(1):13–142.
- McPhie, J., Doyle, M., and Allen, R. L. (1993). Volcanic textures: a guide to the interpretation of textures in volcanic rocks. *Centre for Ore deposit and exploration studies*.
- Meijers, M. (2007). Paleolatitude reconstruction of Upper Permian limestone olistoliths within the Karakaya Complex (Turkey): Eurasia or Gondwana? In *Geophysical Research Abstracts*, volume 9, page 06296.
- Meschede, M. (1986). A method of discriminating between different types of mid-ocean ridge basalts and continental tholeiites with the Nb-Zr-Y diagram. *Chemical geology*, 56(3):207–218.
- Middlemost, E. A. (1994). Naming materials in the magma/igneous rock system. *Earth-Science Reviews*, 37(3):215–224.
- Minařík, L., Žigová, A., Bendl, J., Skřivan, P., and Štastný, M. (1998). The behaviour of rare-earth elements and Y during the rock weathering and soil formation in the Říčany granite massif, Central Bohemia. *Science of the total environment*, 215(1):101–111.
- Moix, P., Beccaletto, L., Kozur, H. W., Hochard, C., Rosselet, F., and Stampfli, G. M. (2008). A new classification of the Turkish terranes and sutures and its implication for the paleotectonic history of the region. *Tectonophysics*, 451(1):7–39.

- Moore, D. M. and Reynolds, R. C. (1989). *X-ray Diffraction and the Identification and Analysis of Clay Minerals*. Oxford University Press, New York. 378p.
- Murton, B. J., Peate, D. W., Arculus, R. J., Pearce, J. A., and van der Laan, S. (1992). Trace element geochemistry of volcanic rocks from site 786: The Izu-Bonin forearc. *Proceedings of the Ocean Drilling Program, Scientific Results*, 125.
- Nesbitt, H. W. (1979). Mobility and fractionation of rare earth elements during weathering of a granodiorite. *Nature*, 279:206–210.
- Nikishin, A., Khotylev, A., Bychkov, A. Y., Kopaevich, L., Petrov, E., and Yapaskurt, V. (2013). Cretaceous volcanic belts and the evolution of the Black Sea basin. *Moscow University Geology Bulletin*, 68(3):141–154.
- Nikishin, A. M., Korotaev, M. V., Ershov, A. V., and Brunet, M.-F. (2003). The Black Sea basin: tectonic history and Neogene–Quaternary rapid subsidence modelling. *Sedimentary Geology*, 156(1):149–168.
- Öhlander, B., Land, M., Ingri, J., and Widerlund, A. (1996). Mobility of rare earth elements during weathering of till in northern Sweden. *Applied Geochemistry*, 11(1):93–99.
- Okay, A., Satır, M., Tüysüz, O., Akyüz, S., and Chen, F. (2001a). The tectonics of the Strandja Massif: Late-Variscan and mid-Mesozoic deformation and metamorphism in the northern Aegean. *International Journal of Earth Sciences*, 90(2):217–233.
- Okay, A., Tüysüz, O., Satır, M., Özkan-Altiner, S., Altiner, D., Sherlock, S., and Eren, R. (2006). Cretaceous and Triassic subduction-accretion, high-pressure–low-temperature metamorphism, and continental growth in the Central Pontides, Turkey. *Geological Society of America Bulletin*, 118(9-10):1247–1269.
- Okay, A. I. (1989). Tectonic units and sutures in the Pontides, northern Turkey. In *Tectonic evolution of the Tethyan region*, pages 109–116. Springer.
- Okay, A. I. (2008). Geology of Turkey. a synopsis. *Anschnitt*, 21:19–42.

- Okay, A. I., Bozkurt, E., Satır, M., Yiğitbaş, E., Crowley, Q. G., and Shang, C. K. (2008). Defining the southern margin of Avalonia in the Pontides: Geochronological data from the Late Proterozoic and Ordovician granitoids from NW Turkey. *Tectonophysics*, 461(1):252–264.
- Okay, A. I., Şengör, A. C., and Görür, N. (1994). Kinematic history of the opening of the Black Sea and its effect on the surrounding regions. *Geology*, 22(3):267–270.
- Okay, A. I. and Tüysüz, O. (1999). Tethyan sutures of northern Turkey. *Geological Society, London, Special Publications*, 156(1):475–515.
- Okay, Aral, I., Tansel, I., and Tüysüz, O. (2001b). Obduction, subduction and collision as reflected in the Upper Cretaceous–Lower Eocene sedimentary record of western Turkey. *Geological Magazine*, 138(02):117–142.
- Pearce, J. (1996). A user's guide to basalt discrimination diagrams. *Geological Association of Canada, Short Course Notes*, 12:79–113. In: Wyman, D.A. (eds) Trace element geochemistry of Volcanic Rocks: Application for Massive Sulphide Exploration.
- Pearce, J. A. (1982). Trace element characteristics of lavas from destructive plate boundaries. *Andesites*, pages 525–548.
- Pearce, J. A. and Cann, J. (1973). Tectonic setting of basic volcanic rocks determined using trace element analyses. *Earth and planetary science letters*, 19(2):290–300.
- Pearce, J. A. and Norry, M. J. (1979). Petrogenetic implications of Ti, Zr, Y, and Nb variations in volcanic rocks. *Contributions to mineralogy and petrology*, 69(1):33–47.
- Peccerillo, A. and Taylor, S. R. (1976). Geochemistry of Eocene calc-alkaline volcanic rocks from the Kastamonu area, northern Turkey. *Contributions to mineralogy and petrology*, 58(1):63–81.
- Pickett, E., , and Robertson, A. H. (1996). Formation of the Late Palaeozoic–Early Mesozoic Karakaya Complex and related ophiolites in NW Turkey by Palaeotethyan subduction–accretion. *Journal of the Geological Society*, 153(6):995–1009.

- Price, R., Gray, C., Wilson, R., Frey, F., and Taylor, S. (1991). The effects of weathering on rare-earth element, Y and Ba abundances in Tertiary basalts from southeastern Australia. *Chemical Geology*, 93(3):245–265.
- Pucéat, E., Lécuyer, C., Sheppard, S. M., Dromart, G., Reboulet, S., and Grandjean, P. (2003). Thermal evolution of Cretaceous Tethyan marine waters inferred from oxygen isotope composition of fish tooth enamels. *Paleoceanography*, 18(2).
- Robertson, A., Dixon, J., Brown, S., Collins, A., Morris, A., Pickett, E., Sharp, I., and Ustaömer, T. (1996). Alternative tectonic models for the Late Palaeozoic-Early Tertiary development of Tethys in the Eastern Mediterranean region. *Geological Society, London, Special Publications*, 105(1):239–263.
- Robertson, A. H. (1998). Tectonic significance of the Eratosthenes seamount: a continental fragment in the process of collision with a subduction zone in the eastern Mediterranean (Ocean Drilling Program Leg 160). *Tectonophysics*, 298(1):63–82.
- Robinson, A., Rudat, J., Banks, C., and Wiles, R. (1996). Petroleum geology of the Black Sea. *Marine and Petroleum Geology*, 13(2):195–223.
- Şahin, S. Y., Aysal, N., and Güngör, Y. (2012). Petrogenesis of Late Cretaceous adakitic magmatism in the Istanbul zone (Çavuşbaşı granodiorite, NW Turkey). *Turkish Journal of Earth Sciences*, 21(6):1029–1045.
- Saribudak, M. (1989). New results and a palaeomagnetic overview of the Pontides in northern Turkey. *Geophysical Journal International*, 99(3):521–531.
- Savov, I. P., Ryan, J. G., D'Antonio, M., Kelley, K., and Mattie, P. (2005). Geochemistry of serpentinized peridotites from the Mariana Forearc Conical Seamount, ODP Leg 125: Implications for the elemental recycling at subduction zones. *Geochemistry, Geophysics, Geosystems*, 6(4).
- Şengör, A. (1985). Strike-slip faulting and related basin formation in zones of tectonic escape: Turkey as a case study. *Special Publication of SEMP*.
- Şengör, A. (1987). Tectonics of the Tethysides: orogenic collage development in a collisional setting. *Annual Review of Earth and Planetary Sciences*, 15:213.

- Şengör, A., Tüysüz, O., Imren, C., Sakinç, M., Eyidogan, H., Görür, N., Le Pichon, X., and Rangin, C. (2005). The North Anatolian fault: A new look. *Annu. Rev. Earth Planet. Sci.*, 33:37–112.
- Şengör, A. and Yilmaz, Y. (1981). Tethyan evolution of Turkey: A plate tectonic approach. *Tectonophysics*, 75(3):181–241.
- Shervais, J. W. (1982). Ti-V plots and the petrogenesis of modern and ophiolitic lavas. *Earth and planetary science letters*, 59(1):101–118.
- Sipahi, F., Sadıklar, M. B., and Şen, C. (2014). Geochemical and Sr–Nd isotopic characteristics of Murgul (Artvin) volcanic rocks in the Eastern Black Sea region (northeast Turkey). *Chemie der Erde-Geochemistry*, 74(3):331–342.
- Stampfli, G. and Borel, G. (2002). A plate tectonic model for the Paleozoic and Mesozoic constrained by dynamic plate boundaries and restored synthetic oceanic isochrons. *Earth and Planetary Science Letters*, 196(1):17–33.
- Stampfli, G. M. (2000). Tethyan Oceans. *Geological Society London, Special publications*, 173(1):1–23.
- Tekeli, O. (1981). Subduction complex of pre-Jurassic age, northern Anatolia, Turkey. *Geology*, 9(2):68–72.
- Trescases, J.-J. (1973). Weathering and geochemical behaviour of the elements of ultramafic rocks in New Caledonia. *Bureau of Mineral Resources Geology and Geophysics Department of Minerals and Energy Canberra Bulletin*, 141:149–161.
- Tüysüz, O. (1999). Geology of the Cretaceous sedimentary basins of the Western Pontides. *Geological Journal*, 34(1-2):75–93.
- Tüysüz, O. (2011). Timing and mechanism of the opening of the Western Black Sea basin. *AAPG Search and Discovery Article*, 30152.
- Tüysüz, O., Dellaloglu, A. A., and Terzioglu, N. (1995). A magmatic belt within the Neotethyan suture zone and its role in the tectonic evolution of northern Turkey. *Tectonophysics*, 243(1):173–191.

- Tüysüz, O., Yilmaz, İ. Ö., Svabenicka, L., and Kirici, S. (2012). The Unaz Formation: A key unit in the Western Black Sea region, N Turkey. *Turkish Journal of Earth Sciences*, 21(6):1009–1028.
- Unal, A., Kamaci, O., YILDIZ, M., ATABEK, G., Yazar, S., and Altunkaynak, S. (2012). Volcanic stratigraphy and petrology of Susurluk volcanites (NW Turkey). *12th International Multidisciplinary Scientific GeoConference SGEM 2012*, 1(12th International Multidisciplinary Scientific GeoConference SGEM2012):391–398.
- Wang, C., Hu, X., Huang, Y., Wagreeich, M., Scott, R., and Hay, W. (2011). Cretaceous Oceanic Red Beds as possible consequence of oceanic anoxic events. *Sedimentary Geology*, 235(1):27–37.
- Winchester, J. and Floyd, P. (1976). Geochemical magma type discrimination: application to altered and metamorphosed basic igneous rocks. *Earth and Planetary Science Letters*, 28(3):459–469.
- Winchester, J. and Floyd, P. (1977). Geochemical discrimination of different magma series and their differentiation products using immobile elements. *Chemical geology*, 20:325–343.
- Wood, D. A. (1980). The application of a Th-Hf -Ta diagram to problems of tectonomagmatic classification and to establishing the nature of crustal contamination of basaltic lavas of the British Tertiary Volcanic Province. *Earth and planetary science letters*, 50(1):11–30.
- Yilmaz, İ. Ö. (2008). Cretaceous pelagic red beds and black shales (Aptian-Santonian), NW Turkey: global oceanic anoxic and oxic events. *Turkish Journal of Earth Sciences*, 17(2):263–296.

A. Abbreviations

Table A.1.: Abbreviations used in the text and/or figures

CAB	calc-alkaline basalt
CRB	continental rift basalt
E-MORB	enriched mid-oceanic ridge basalt
IAB	island arc basalt
IAT	island arc tholeiite
MORB	mid-oceanic ridge basalt
N-MORB	normal mid-oceanic ridge basalt
OFB	ocean floor basalt
P-MORB	plume-influenced mid-ocean-ridge basalt
VAB	volcanic arc basalt
WPA	within-plate alkaline basalt
WPB	within-plate basalt
WPT	within-plate tholeiite

B. Tables

Table B.1.: Coordinates of the outcrops visited alongside the SW Black Sea coast

Outcroplist - Western Pontides 2013

Outcrop No#	Coordinates			Tuff samples
	N	E		
T13- 01	41°54.865'	033°01.629'	E of Cide, Köseli	T13/03/T
T13- 02	41°55.789'	033°04.151'	Kuscu	T13/11b/T T13/12/T T13/12b/T
T13- 03	41°56.860'	033°08.524'	Camalti	
T13- 04	41°58.661'	033°13.135'	Akbayir	
T13- 05	41°59.780'	033°16.738'	Alayazi	T13/16/T
T13- 06	41°51.691'	032°51.999'	Gideros	
T13- 07	41°51.478'	032°51.375'	Gideros	
T13- 08	41°50.926'	032°45.773'	Kapisuyu	
T13- 09	41°48.955'	032°40.194'	Cayalti (near Unaz village)	T13/28/T T13/30a/T T13/30b/T
T13- 10	41°49.681'	032°37.202'	Karaman	
T13- 11	41°48.924'	032°35.815'	Meydan / Unaz village	
T13- 12	41°44.121'	032°25.851'	Inpiri	
T13- 13	41°44.266'	032°25.652'	E of Amasra (road exit Amasra)	T13/34/T
T13- 14	41°44.116'	032°22.183'	W of Amasra	
T13- 15	41°43.649'	032°22.210'	Gömü	
T13- 16	41°43.553'	032°22.083'		
T13- 17	41°41.145'	032°21.723'	Kaman	T13/37/T T13/37b/T
T13- 18	41°41.490'	032°23.266'	Ugurlar	T13/38/T T13/39/T
T13- 19	41°43.884'	032°24.774'	SE of Amasra D010	T13/40/T
T13- 20	41°43.697'	032°25.119'	SE of Amasra D010	
T13- 21	41°44.197'	032°24.646'	Amasra	T13/42/T
T13- 22	41°39.205'	032°21.423'	East of Bartin	T13/48/T
T13- 23	41°39.047'	032°21.464'	East of Bartin	
T13- 24	41°39.626'	032°20.516'	Uzunöz	
T13- 25	41°38.843'	032°21.491'	East of Bartin	

Table B.3.: Overview of geochemical classification results

sample	Classification according to											Element variations - specials	
	TAS (LeBas et al., 1986)	TAS (Middlemost, 1994)	Nb/Y-Zr/Ti (Winchester and Floyd, 1977)	Nb/Y-Zr/TiO2 (Pearce, 1996)	Th-Co (Hastie et al., 2007)	K2O-SiO2 (Peccerillo and Taglior, 1976)	Th/Yb-Ta/Yb (Pearce, 1982)	Th-Co (Hastie et al., 2007)	Element variations (norm. to MMORB)	Ti-Zr-Y (Pearce and Cann, 1973)	Zr/Hf-Ta (Meschede, 1986)		Th-Hf-Ta (Wood, 1980)
37b	Ba	Ba	And/Ba	Ba	Ba	h.k.	c.a.	c.a.	MORB/CABIAT	VABINMORB	CAB/YAB	Island Arc Basalt	
38	Ba	Ba	And/Ba	Ba	Ba	h.k.	c.a.	c.a.	MORB/CABIAT	VABINMORB	CAB/YAB	Island Arc Basalt	
28	Foidite	Foidite	And/Ba	Ba	Ba/And-And	shos	c.a.	th	MORB/CABIAT	VABINMORB	CAB/YAB	Island Arc Basalt	
30a	Ba/And	Ba/And	And/Ba	Ba	Ba/And-And	h.k.	c.a.	th	MORB/CABIAT	VABINMORB	CAB/YAB	Island Arc Basalt	
30b	TE	TE	And/Ba	Ba	Ba/And-And	shos	c.a.	th	MORB/CABIAT	VABINMORB	CAB/YAB	Island Arc Basalt	
03	And	And	And/Ba	Ba	Ba/And-And	shos	c.a.	c.a. - h.k.	MORB/CABIAT	VABINMORB	CAB/YAB	Island Arc Basalt	
34	And	And	And/Ba	Ba	Ba/And-And	h.k.	shos	c.a. - h.k.	MORB/CABIAT	VABINMORB	CAB/YAB	Island Arc Basalt	
12b	Ba	Ba	And/Ba	Ba	Ba/And-And	shos	c.a.	c.a. - h.k.	CAB	VAB	CAB/YAB	Island Arc Basalt	more Nb
12	Ba	Ba	And	And-Ba/And	Ba/And-And	shos	shos	c.a. - h.k.	CAB	VAB	CAB/YAB	Island Arc Basalt	
39	Ba/And	Ba/And	And/Ba	And-Ba/And	Ba/And-And	shos	shos	c.a. - h.k.	CAB	VAB	CAB/YAB	Island Arc Basalt	
40	And	And	DaRly	And-Ba/And	Ba/And-And	c.a.	shos	c.a. - h.k.	CAB	VAB	CAB/YAB	Island Arc Basalt	more Zr
37	And	And	DaRly	And-Ba/And	Ba/And-And	c.a.	shos	c.a. - h.k.	-	-	CAB/YAB	Island Arc Basalt	more Zr
11b	Foidite	Foidite	And/Ba	Ba	DaRly	shos	shos	c.a. - h.k.	CAB	VAB	CAB/YAB	Island Arc Basalt	
48	Foidite	Foidite	And	And-Ba/And	DaRly	shos	shos	c.a. - h.k.	CAB	VAB	CAB/YAB	Island Arc Basalt	
16	low SiO2	Foidite	And/Ba	Ba	DaRly	shos	shos	th	WPB	VAB	CAB/YAB	Island Arc Basalt	
42	Dacite	Dacite	DaRly	DaRly	DaRly	th	shos	c.a. - h.k.	-	WPA	CAB/YAB	Island Arc Basalt	less TiO2
And	Andesite	Andesite				alk	alk/alkine		CAB				calc-alk/alkine basalt
Ba	Basalt	Basalt				c.a.	calc/alk/alkine		IA7				island arc tholeiit
Ba/And	Basaltic Andesite	Basaltic Andesite				Alk	high K/ calc/alk/alkine		MORB				mid-ocean ridge basalt
DaRly	Dacite/Rhyolite	Dacite/Rhyolite				shos	shoshonitic		MORB				tholeiitic/MORB
FG	Ficobasalt	Ficobasalt				sub a-th	subalk/alkine - tholeiitic		YAB				volcanic arc basalt
TE	(basaltic)/Trachybasalt	(basaltic)/Trachybasalt				th	tholeiitic		WPA				within plate alk/alk basalt
									WPA				within plate basalt

C.

CURRICULUM VITAE

NAME	KATHARINA BÖHM
UNIVERSITY AND SCHOOL EDUCATION	
Since 10/2012	Master program of Earth Science at University of Vienna Master's thesis: "Late Cretaceous Volcaniclastic Rocks in the Western Pontides (NW Turkey)"
10/2009 – 10/2012	Bachelor program of Earth Science at University of Vienna Bachelor's thesis: "Serpentinite slices on the eastern edge of the Eastern Alps – part of Meliaticum?"
09/2004 - 06/2009	Higher level commercial school, <i>Bundeshandelsakademie Neunkirchen</i> (Austria), Specialization International Economy: graduation with "with excellence"
Special Courses at University	<ul style="list-style-type: none">- Mapping courses (Schönfeld/Salzburg, Weyer/Upper Austria, Ötztal/Tyrol, Stubaital/Tyrol)- Structural geology Field course (Zillertal/Tyrol)- Mineralogical Field courses (Pegmatites/Erzgebirge, REE Pegmatites/Kola, Alluvial Gems/Sri Lanka)- Geologic Field trip to Scotland, Eifel/Germany
Laboratory and Analytical Skills	Whole rock powder X-ray diffractometry(XRD) Whole rock powder X-ray fluorescence (XFA) Raman and IR-spectroscopy course Geochronology course Mineral identification with polarization microscopy and reflected light microscopy Sedimentological Analysis including clay mineral analysis

WORK EXPERIENCE

Geological Survey Austria

- Geological mapping in wine-growing area with hand sampled cores (Autumn/Winter 2014/2015)
- Participation in "GeoloGIS" project (Spring 2013)
New database of outcrops and boreholes in Upper Austria, request: Federal State Government Upper Austria
- Hydrological detailed mapping - Bucklige Welt/Lower Austria(August 2012)

Fronterra Geoscience

Internship, August and September 2013
Resistivity Log interpretation, OMV Project Tunisia

European Geosciences
Union

Student Assistant at EGU General Assembly, 2010-2015

University of Vienna

Tutorships at University exercise courses:
- Mapping Course Ötztal/Tyrol (2013)
- Actuo-Palontological course Friuli/Italy (2013)
- Earth History and Stratigraphy (2010-2011, 2011-2012)

CONFERENCE CONTRIBUTION

- European General Assembly 2015
Poster presentation: Late Cretaceous Volcaniclastics in NW Turkey.
- Pangeo Austria 2014
Poster contribution: Biostratigraphy, palaeoecology and geochemistry of tuffs - an integrated study of three Upper Cretaceous sections in the Western Pontides, NW Turkey.
- European General Assembly 2014
Poster presentation (new approaches): Serpentinite slices within a tectonic zone at the base of the Juvavic nappe system in the Northern Calcareous Alps (Austria): characterization and origin.
- Emile Argand Conference on Alpine Geological Studies, Schladming 2013
Poster presentation: Serpentinite slices within a tectonic zone at the base of the Juvavic nappe system (Eastern Alps, Austria): Petrography and Geochemistry.

PUBLICATIONS

Publication in Austrian Journal of Earth Science in preparation (next issue): Serpentinite Slices in a tectonic zone at the base of Juvavic nappe system in the Eastern Alps: Characterization and Origin

RESEARCH INTERESTS

Petrology, Geochemistry
Geochronology and Isotopes